

University of Windsor

## Scholarship at UWindor

---

Electronic Theses and Dissertations

Theses, Dissertations, and Major Papers

---

2014

# Design of System Architecture and Thermal Management Components for an Underwater Energy Storage Facility

Brian C. Cheung  
*University of Windsor*

Follow this and additional works at: <https://scholar.uwindsor.ca/etd>



Part of the [Civil and Environmental Engineering Commons](#)

---

### Recommended Citation

Cheung, Brian C., "Design of System Architecture and Thermal Management Components for an Underwater Energy Storage Facility" (2014). *Electronic Theses and Dissertations*. 5065.  
<https://scholar.uwindsor.ca/etd/5065>

This online database contains the full-text of PhD dissertations and Masters' theses of University of Windsor students from 1954 forward. These documents are made available for personal study and research purposes only, in accordance with the Canadian Copyright Act and the Creative Commons license—CC BY-NC-ND (Attribution, Non-Commercial, No Derivative Works). Under this license, works must always be attributed to the copyright holder (original author), cannot be used for any commercial purposes, and may not be altered. Any other use would require the permission of the copyright holder. Students may inquire about withdrawing their dissertation and/or thesis from this database. For additional inquiries, please contact the repository administrator via email ([scholarship@uwindsor.ca](mailto:scholarship@uwindsor.ca)) or by telephone at 519-253-3000ext. 3208.

# Design of System Architecture and Thermal Management Components for an Underwater Energy Storage Facility

by

Brian C. Cheung

A Thesis

Submitted to the Faculty of Graduate Studies

through the Department of Civil and Environmental Engineering

in Partial Fulfilment of the Requirements for

the Degree of Master of Applied Science at the

University of Windsor

Windsor, Ontario, Canada

© 2014 Brian C. Cheung

**DESIGN OF SYSTEM ARCHITECTURE AND THERMAL  
MANAGEMENT COMPONENTS FOR AN UNDERWATER  
ENERGY STORAGE FACILITY**

by

Brian C. Cheung

APPROVED BY:

---

Dr. Andrzej Sobiesiak

Department of Mechanical, Automotive & Materials Engineering

---

Dr. Sreekanta Das

Department of Civil and Environmental Engineering

---

Dr. Rupp Carriveau, Advisor

Department of Civil and Environmental Engineering

---

Dr. David S-K. Ting, Co-Advisor

Department of Mechanical, Automotive & Materials Engineering

December 12, 2013

## DECLARATION OF CO-AUTHORSHIP/PREVIOUS PUBLICATIONS

I hereby declare that this thesis incorporates material that is result of joint research, as follows:

| <b>Thesis Chapter</b> | <b>Details</b>  |
|-----------------------|---|
| Chapter 2             | This thesis incorporates the outcome of a joint research project undertaken in collaboration with Mr. Ning Cao under the supervision of Dr. Rupp Carriveau and Dr. David S-K. Ting. In all cases, the author performed the key ideas, primary contributions and data analysis and interpretation, and the contribution of the co-author was primarily through the provision of developing experimental designs and data collection. |

I am aware of the University of Windsor Senate Policy on Authorship and I certify that I have properly acknowledged the contribution of other researchers to my thesis, and have obtained written permission from each of the co-author(s) to include the above material(s) in my thesis.

I certify that, with the above qualification, this thesis, and the research to which it refers, is the product of my own work.

This thesis includes three original papers that have been previously published/submitted for publication in peer reviewed journals, as follows:

| <b>Thesis Chapter</b> | <b>Publication</b>   | <b>Publication status</b> |
|-----------------------|--|---------------------------|
| Chapter 2             | B. Cheung, N. Cao, R. Carriveau, and D. S.-K. Ting, "Distensible air accumulators as a means of adiabatic underwater compressed air energy storage," International Journal of Environmental Studies, vol. 69, no. 4, pp. 566–577, Aug. 2012. | Published                 |
| Chapter 3             | B. Cheung, R. Carriveau & D. S-K. Ting, "Parameters affecting scalable underwater compressed air energy storage," Applied Energy   | Under review              |

| <b>Thesis Chapter</b> | <b>Publication</b>   | <b>Publication status</b> |
|-----------------------|--|---------------------------|
| Chapter 4             | B. Cheung, R. Cariveau & D. S.-K. Ting, “Multi-objective optimization of an underwater compressed air energy storage system using a genetic algorithm,” Energy | Submitted                 |

I certify that I have obtained a written permission from the copyright owner(s) to include the above published material(s) in my thesis. I certify that the above material describes work completed during my registration as a graduate student at the University of Windsor.

I declare that, to the best of my knowledge, my thesis does not infringe upon anyone’s copyright nor violate any proprietary rights and that any ideas, techniques, quotations, or any other material from the work of other people included in my thesis, published or otherwise, are fully acknowledged in accordance with the standard referencing practices. Furthermore, to the extent that I have included copyrighted material that surpasses the bounds of fair dealing within the meaning of the Canada Copyright Act, I certify that I have obtained a written permission from the copyright owner(s) to include such material(s) in my thesis.

I declare that this is a true copy of my thesis, including any final revisions, as approved by my thesis committee and the Graduate Studies office, and that this thesis has not been submitted for a higher degree to any other University or Institution.

## ABSTRACT

The electricity industry is currently experiencing a significant paradigm shift in managing electrical resources. With the onset of aging infrastructure and growing power demands, and the influx of intermittent renewable energy generation, grid system operators are looking towards energy storage as a solution for mitigating industry challenges. An emerging storage solution is underwater compressed air energy storage (UWCAES), where air compressors and turbo-expanders are used to convert electricity to and from compressed air stored in submerged accumulators. This work presents three papers that collectively focus on the design and optimization of an UWCAES system. In the first paper, the field performance of a distensible air accumulator is studied for application in UWCAES systems. It is followed by a paper that analyzed the energetic and exergetic performance of a theoretical UWCAES system. The final paper presents a multi-objective UWCAES optimization model utilizing a genetic algorithm to determine optimum system configurations.

## DEDICATION

This work is dedicated to my maker and saviour whom by grace, through faith, redeemed my soul and guides my life and to my parents for their love, support, and sacrifice in my upbringing.

## ACKNOWLEDGEMENTS

I would like to acknowledge the leadership, wisdom, and support provided by my primary advisor, Dr. Rupp Carriveau, and co-advisor, Dr. David S-K. Ting. The guidance and patience they have given me has been essential throughout the past two years and has helped me grow. I would also like to thank Dr. Sreekanta Das and Dr. Andrzej Sobiesiak for their contributions in providing their time and knowledge to keep me on track in my master's project. As well, I would like to acknowledge the contributions of Mr. Ning Cao who set up and conducted the pilot project discussed in Chapter 2 of this thesis. Additionally, I would like to thank Dr. Hanna Maoh for his contributions to my thesis defense. Finally, I would like to acknowledge Mr. Cameron Lewis and Mr. Curtis VanWalleghem of Hydrostor, for the opportunity to have been part of the team developing the world's first underwater compressed air energy system.

The Ontario Centres of Excellence and Sustainable Development Technology Canada have also supported this work.



A Turbulence & Energy Lab  
Research Project



## TABLE OF CONTENTS

|  |      |
|--|------|
| Declaration of Co-Authorship/Previous Publications .....   | iii  |
| Abstract .....   | v    |
| Dedication .....   | vi   |
| Acknowledgements.....  | vii  |
| List of Tables.....  | xii  |
| List of Figures .....  | xiii |
| Chapter I .....  | 1    |
| Introduction .....   | 1    |
| 1.0 Background .....   | 1    |
| 2.0 Methodology .....  | 3    |
| References .....   | 6    |
| Chapter II.....  | 8    |
| Distensible air accumulators as a means of adiabatic underwater compressed air<br>energy storage ..... | 8    |
| Nomenclature.....  | 8    |
| 1.0 Introduction .....   | 9    |
| 1.1 The reason for energy storage.....   | 9    |
| 1.2 Conventional Compressed Air Energy Storage .....   | 10   |
| 1.3 CAES technology in practice .....  | 11   |
| 2.0 Underwater Compressed Air Energy Storage.....  | 12   |
| 2.1 Benefits of UWCAES .....   | 14   |

|             |   |    |
|-------------|---|----|
| 2.2         | UWCAES Configuration .....  | 15 |
| 3.0         | UWCAES Pilot Project.....   | 19 |
| 3.1         | Experimentation .....   | 19 |
| 3.2         | Results .....   | 20 |
| 3.3         | Discussion.....   | 23 |
| 4.0         | Conclusions.....  | 24 |
|             | Acknowledgements .....  | 24 |
|             | References .....  | 24 |
| Chapter III | .....   | 27 |
|             | Parameters affecting scalable underwater compressed air energy storage..... | 27 |
|             | Nomenclature.....   | 27 |
| 1.0         | Introduction .....  | 28 |
| 2.0         | Underwater Compressed Air Energy Storage.....                               | 29 |
| 3.0         | System Modelling .....  | 33 |
| 3.1         | Design Theory.....  | 33 |
| 3.2         | Configuration .....   | 36 |
| 3.3         | Methodology.....  | 38 |
| 4.0         | Results and Discussion.....   | 40 |
| 5.0         | Conclusions .....   | 46 |
|             | Acknowledgements .....  | 47 |
|             | References .....  | 47 |
| Chapter IV  | .....   | 51 |

|   |    |
|---|----|
| Multi-objective optimization of an underwater compressed air energy storage system<br>using a genetic algorithm ..... | 51 |
| Nomenclature.....   | 51 |
| 1.0 Introduction .....  | 52 |
| 2.0 Simulating & Analyzing UWCAES .....   | 55 |
| 2.1 Thermal Performance.....  | 56 |
| 2.2 Exergy Analysis .....   | 58 |
| 2.3 Exergoeconomic Analysis .....   | 59 |
| 3.0 Multi-objective Genetic Algorithm Optimization.....   | 61 |
| 3.1 Optimization Process.....   | 62 |
| 3.2 Multiple Criterion Decision Making.....   | 64 |
| 4.0 Case Study.....   | 65 |
| 4.1 Modelling Approach .....  | 65 |
| 4.2 System Variables .....  | 66 |
| 4.3 Cost Functions.....   | 67 |
| 4.4 Optimization Objectives .....   | 69 |
| 4.5 Modelling and Optimization Considerations.....  | 69 |
| 5.0 Results.....  | 70 |
| 6.0 Conclusions.....  | 74 |
| Acknowledgements .....  | 74 |
| References .....  | 74 |
| Chapter V .....   | 79 |

|   |    |
|---|----|
| Conclusions and Recommendations .....                         | 79 |
| 1.0 Summary and Conclusions .....                             | 79 |
| 2.0 Recommendations.....                                      | 80 |
| Appendix A.....   | 82 |
| Permissions for previously published works .....              | 82 |
| Appendix B.....   | 83 |
| Performance Evaluation of Preferred System Configuration..... | 83 |
| Vita Auctoris .....   | 88 |

## LIST OF TABLES

### **CHAPTER III: PARAMETERS AFFECTING SCALABLE UNDERWATER COMPRESSED AIR ENERGY STORAGE**

|                                     |    |
|-------------------------------------|----|
| Table 1 – Baseline values.....      | 38 |
| Table 2 – Parameter variation ..... | 39 |

### **CHAPTER IV: MULTI-OBJECTIVE OPTIMIZATION OF AN UNDERWATER COMPRESSED AIR ENERGY STORAGE SYSTEM USING A GENETIC ALGORITHM**

|  |    |
|--|----|
| Table 1 – Decision variables.....  | 66 |
| Table 2 – Additional analysis variables .....  | 67 |
| Table 3 – Equipment cost functions .....   | 68 |
| Table 4 – Summary of objective functions .....   | 69 |
| Table 5 – Selected system design summary at different interest rates .....             | 73 |
| Table 6 – Performance of the selected system designs at different interest rates ..... | 73 |

### **APPENDIX B: PERFORMANCE EVALUATION OF PREFERRED SYSTEM CONFIGURATION**

|  |    |
|--|----|
| Table B-1 – Energy Analysis of Modelled System .....                               | 84 |
| Table B-2 – Exergy Analysis of Modelled System .....                               | 85 |
| Table B-3 – Exergoeconomic Analysis of Modelled System (Cost Per Unit Exergy)..... | 86 |
| Table B-4 – Exergoeconomic Analysis of Modelled System (Cost Rate) .....           | 87 |

## LIST OF FIGURES

### **CHAPTER II: DISTENSIBLE AIR ACCUMULATORS AS A MEANS OF ADIABATIC UNDERWATER COMPRESSED AIR ENERGY STORAGE**

|  |    |
|--|----|
| Figure 1 – Traditional CAES process .....                    | 11 |
| Figure 2 – Illustration of a UWCAES system .....             | 13 |
| Figure 3 – UWCAES system layout .....                        | 15 |
| Figure 4 – Experimental configuration of pilot project ..... | 20 |
| Figure 5 – Accumulator discharge data .....                  | 21 |
| Figure 6 – Accumulator charge data .....                     | 22 |

### **CHAPTER III: PARAMETERS AFFECTING SCALABLE UNDERWATER COMPRESSED AIR ENERGY STORAGE**

|  |    |
|--|----|
| Figure 1 – UWCAES process diagram .....  | 30 |
| Figure 2 – A land-based UWCAES system .....  | 30 |
| Figure 3 – An UWCAES system located on an off-shore barge .....  | 31 |
| Figure 4 – UWCAES among other EES technologies .....   | 32 |
| Figure 5 – Relative change in round-trip efficiency and total exergy<br>destruction due to parameter variation ..... | 41 |
| Figure 6 – Mass vs. depth .....  | 41 |
| Figure 7 – Component contribution to total exergy destruction .....  | 42 |
| Figure 8 – Extent of deviation in round-trip efficiency and total exergy<br>destruction from baseline .....          | 43 |

|  |    |
|--|----|
| Figure 9 – Sensitivity of round-trip efficiency, total exergy destruction<br>to design parameters..... | 44 |
| Figure 10 – Sensitivity of system component exergy destruction to<br>design parameters.....            | 45 |

#### **CHAPTER IV: MULTI-OBJECTIVE OPTIMIZATION OF AN UNDERWATER COMPRESSED AIR ENERGY STORAGE SYSTEM USING A GENETIC ALGORITHM**

|  |    |
|--|----|
| Figure 1 – The general UWCAES process.....                       | 56 |
| Figure 2 – The basic process flow of a genetic algorithm .....   | 62 |
| Figure 3 – A Pareto-optimal front .....                          | 63 |
| Figure 4 – A UWCAES system with on-shore equipment .....         | 65 |
| Figure 5 – Average hourly electricity prices over 24-hours ..... | 68 |
| Figure 6 – Pareto-optimal solutions (IR = 10%) .....             | 70 |
| Figure 7 – Total cost rate vs. round-trip efficiency .....       | 71 |
| Figure 8 – Operating profit vs. total cost rate .....            | 71 |
| Figure 9 – Pareto-optimal solutions (IR = 5% to 15%) .....       | 72 |

# CHAPTER I

## INTRODUCTION

### 1.0 BACKGROUND

Energy storage is of ever increasing interest to the electricity market as the growing need for energy places a greater strain on existing, aging grid assets. The capacity to store large amounts of energy for consumption at a later time provides many advantages to grid users and operators. Energy businesses can capitalize on fluctuating energy markets through energy arbitrage – buying and storing when electricity prices are low and generating and selling when demand and prices are high.

The benefits of storage are evident, summarized in [1]. Storage allows for a reduction in power transmission and distribution congestion; which improves existing grid efficiency and can reduce costs for sellers trying to get their energy product to market. Storage can also significantly increase the utilization of existing generation assets. Generation facilities that would not normally generate during non-peak time can continue to generate past peak, storing the excess for use when required. Storage is particularly valuable for intermittent generators like wind and solar; energy storage has great potential in transforming these renewable energy supplies into dispatchable generation assets by storing energy produced in times of high supply and delivering it on demand.

An emerging technology in the field of energy storage is underwater compressed air energy storage (UWCAES). Using a series of air compressors and turbo-expanders, electricity is converted to and from electricity. UWCAES builds on the established foundations of traditional compressed air energy storage (CAES), while incorporating thermal energy storage and scalable air storage reservoirs. The novelty of the UWCAES



concept lies in the air storage method – using submerged, distensible air accumulators. The accumulators are placed at or near the bedding of deep water bodies and rely on the hydrostatic pressure exerted by the surrounding water. The compressed air maintains its pressure in the accumulators, as the storage volume can vary based on filled capacity.

The research objectives of this thesis are as follows:

- To establish the necessary components of a full-scale UWCAES system,
- To understand design parameter influence on UWCAES system performance and highlight ways of improving performance with methods yielding the greatest benefit, and
- To determine optimal configurations of a UWCAES system for a given set of constraints.

A survey of available literature shows limited research into UWCAES, as well as alternative CAES methods that provide characteristics similar to UWCAES. For the UWCAES concept, research to date has primarily focused on the distensible accumulator element, with studies examining its shape [2,3] and hydrodynamic flow interaction [4]. There have been few studies that sought to achieve characteristics similar to UWCAES, particularly to design CAES systems that are isobaric and/or scalable. In [5], a water-compensated, geologic CAES system was analyzed that featured a water head supplied by an aboveground water reservoir; the water head was used to achieve isobaric performance. Scalability of CAES systems has been examined by researchers using aboveground pressure vessels [6–8] and steel pipe piles [9].

As well, tools such as exergy and exergoeconomic analyses, which provide valuable insights into the thermodynamic operation of systems, have been sparsely applied to CAES thus far. As exergy measures work potential and quantifies energy quality, its assessment can help identify the location and magnitude of losses in a system.

An analysis of the system is further enhanced by exergoeconomics, which assigns cost information to system exergy. While these analysis methods, in general, have gained significant attention, only a handful of publications applying these analyses to CAES exist; studies of exergy in CAES systems can be found in [5,6,10,11], whereas [12,13] incorporated exergoeconomic evaluation.

These publications show the extent in which general CAES system design and performance research has been applied to. As both energy demand and costs increase, sustainability becomes an important consideration for energy systems. This thesis attempts to address the issue of sustainability in CAES systems, particularly UWCAES, through the optimization of its design parameters. It studies the application of energy, exergy, and exergoeconomic analysis in a multi-objective optimization model to determine optimal system configurations. While multi-objective optimization techniques have been applied in analyzing thermal energy systems, such as combined cycle power systems, such techniques have yet to be applied to CAES systems.

## **2.0 METHODOLOGY**

For the UWCAES concept to be established, it is important that its performance as a system and on a component-basis is understood. The concept is first introduced in Chapter 2 and provides a discussion of the working principles of UWCAES and its advantages over conventional CAES systems. Following the discussion, results and findings from a field demonstration of a scaled-down distensible air accumulator is presented. The pilot project, conducted in September 2011 in Lake Ontario, consisted of a submerged, distensible air accumulator placed at a depth approximately 30 m below the water surface. The air accumulator and was connected to an air compressor situated onshore by a 1 km-long rubber hose. Using the air compressor, the charge and discharge performance of the accumulator were studied to assess its feasibility for use in an

UWCAES system. The results of the pilot project validated the proof-of-concept of the accumulator element in UWCAES.

Chapter 3 focused on evaluating the performance of a theoretical UWCAES system to determine the impact design parameters may have on system operation. Major system components were numerically modelled and individually evaluated for energy and exergy. This was done in order to locate and quantify the magnitude of losses in the UWCAES process. The system model, rated for a power output of 4 MWh, consisted of three air compression stages, three air expansion stages, three heat exchangers, a thermal storage reservoir, and an air delivery header pipe connected to a variable number of air accumulators. A parametric study of the modelled system examined the following design parameters:

1. Air storage depth,
2. Off-shore distance,
3. System power input,
4. Compressor isentropic efficiency,
5. Maximum heat exchanger extraction temperature ratio,
6. Thermal storage insulation thickness,
7. Air delivery header pipe diameter,
8. Expander isentropic efficiency, and
9. Charge-to-discharge time ratio.

In the parametric study, the performance of the system was expressed by two quantities – system round-trip efficiency and total exergy destruction. The results of the parametric study were used in a sensitivity analysis to determine parameter significance on system performance. The findings of the sensitivity analysis demonstrated the 4

significance parameters: air delivery header pipe diameter, expander isentropic efficiency, compressor isentropic efficiency, and air storage depth.

Building on the research performed using the parametric study and sensitivity analysis, Chapter 4 sought to determine optimal system configurations by means of a multi-objective optimization model. In addition to analyzing energy and exergy, this study integrated exergoeconomic analysis in order to assign cost information to system losses. An improved numerical UWCAES model was developed simulating a 4 MWh on-shore system with air storage situated 5 km off-shore and 100 m below the water surface in a fresh water lake. This model was subjected to various system configurations based on the following design parameters:

1. System power input,
2. Number of air compression stages,
3. Air delivery header pipe diameter,
4. Number of air expansion stages, and
5. Charge-to-discharge time ratio.

Every component in each configuration was evaluated for energy, exergy and exergoeconomics – firstly, the operational performance was quantified; secondly, the exergy rates and destruction was determined; thirdly, the cost per unit exergy was calculated for every exergy stream; and finally, the cost rate of every exergy stream, including exergy destruction, was priced. Equipment capital cost functions, based on functions sourced from literature and adjusted by economic cost indices provided by the United States Bureau of Labor Statistics and quotes sourced from equipment manufactures, were used in the calculation of exergy stream cost rates.

Three distinct optimization objective functions were developed from the thermodynamic and exergoeconomic analyses, which calculated the system's round-trip

efficiency, the total cost rate of exergy destruction and capital costs, and operating profit per cycle. These functions were applied in a multi-objective optimization model that used the elitist non-dominated sorting genetic algorithm (NSGA-II) method to determine optimal configurations based on the supplied information. In addition, the impact of interest rates on optimal system designs was gauged using a sensitivity analysis. A multi-criterion decision making approach was employed on the optimization results which selected a preferred design at the different interest rates examined. The detailed results of the energy, exergy, exergoeconomic analyses of the preferred system can be found in Appendix B.

These analysis performed in this thesis sets a foundation for building future UWCAES systems and further research on improving their performance. The research presented herein can be improved using more advanced system models and better cost estimates. As electrical energy management methods evolve moving forward, energy storage systems will proliferate. The analysis prescribed in this thesis serve to achieve future energy sustainability.

## REFERENCES

- [1] J. Eyer and G. Corey, "Energy Storage for the Electricity Grid: Benefits and Market Potential Assessment Guide," Sandia National Laboratories, 2010.
- [2] A. Pimm and S. Garvey, "Analysis of flexible fabric structures for large-scale subsea compressed air energy storage," *J. Phys. Conf. Ser.*, vol. 181, no. 1, p. 012049, Aug. 2009.
- [3] A. J. Pimm, S. D. Garvey, and R. J. Drew, "Shape and cost analysis of pressurized fabric structures for subsea compressed air energy storage," *Proc. Inst. Mech. Eng. Part C J. Mech. Eng. Sci.*, vol. 225, no. 5, pp. 1027–1043, May 2011.
- [4] A. R. Vassel-Be-Hagh, R. Carriveau, and D. S.-K. Ting, "Numerical simulation of flow past an underwater energy storage balloon," *Comput. Fluids*, vol. 88, pp. 272–286, 2013.

- [5] Y. M. Kim, D. G. Shin, and D. Favrat, "Operating characteristics of constant-pressure compressed air energy storage (CAES) system combined with pumped hydro storage based on energy and exergy analysis," *Energy*, vol. 36, no. 10, pp. 6220–6233, Nov. 2011.
- [6] Y. M. Kim and D. Favrat, "Energy and exergy analysis of a micro-compressed air energy storage and air cycle heating and cooling system," *Energy*, vol. 35, no. 1, pp. 213–220, Jan. 2010.
- [7] H. Ibrahim, R. Younès, A. Ilinca, M. Dimitrova, and J. Perron, "Study and design of a hybrid wind–diesel-compressed air energy storage system for remote areas," *Appl. Energy*, vol. 87, no. 5, pp. 1749–1762, May 2010.
- [8] J. J. Proczka, K. Muralidharan, D. Villela, J. H. Simmons, and G. Frantziskonis, "Guidelines for the pressure and efficient sizing of pressure vessels for compressed air energy storage," *Energy Convers. Manag.*, vol. 65, pp. 597–605, Jan. 2013.
- [9] L. Zhang, S. Ahmari, M. Budhu, and B. Sternberg, "Feasibility Study of Compressed Air Energy Storage Using Steel Pipe Piles," in *GeoCongress 2012*, 2012, pp. 4272–4279.
- [10] G. Grazzini and A. Milazzo, "A Thermodynamic Analysis of Multistage Adiabatic CAES," *Proc. IEEE*, vol. 100, no. 2, pp. 461–472, Feb. 2012.
- [11] Y.-M. Kim, J.-H. Lee, S.-J. Kim, and D. Favrat, "Potential and Evolution of Compressed Air Energy Storage: Energy and Exergy Analyses," *Entropy*, vol. 14, no. 12, pp. 1501–1521, Aug. 2012.
- [12] F. Buffa, S. Kemble, G. Manfrida, and A. Milazzo, "Exergy and Exergoeconomic Model of a Ground-Based CAES Plant for Peak-Load Energy Production," *Energies*, vol. 6, no. 3, pp. 1050–1067, Feb. 2013.
- [13] A. Bagdanavicius and N. Jenkins, "Exergy and exergoeconomic analysis of a Compressed Air Energy Storage combined with a district energy system," *Energy Convers. Manag.*, vol. 77, pp. 432–440, Jan. 2014.

## CHAPTER II<sup>1</sup>

# **DISTENSIBLE AIR ACCUMULATORS AS A MEANS OF ADIABATIC UNDERWATER COMPRESSED AIR ENERGY STORAGE**

BRIAN CHEUNG<sup>†</sup>, NING CAO<sup>‡</sup>, RUPP CARRIVEAU<sup>†2</sup>, DAVID S-K TING<sup>‡</sup>

<sup>†</sup>Department of Civil and Environmental Engineering, University of Windsor, Windsor, Ontario, Canada;

<sup>‡</sup>Department of Mechanical Automotive and Materials Engineering, University of Windsor, Windsor, Ontario, Canada

B. Cheung, N. Cao, R. Cariveau, and D. S.-K. Ting, “Distensible air accumulators as a means of adiabatic underwater compressed air energy storage,” *International Journal of Environmental Studies*, vol. 69, no. 4, pp. 566–577, Aug. 2012.

## **NOMENCLATURE**

|            |   |           |                              |
|------------|---|-----------|------------------------------|
| $E$        | Energy                                  | $V_{bag}$ | Volume of an air accumulator |
| $m$        | Mass                                    | $v$       | Specific volume              |
| $N_{bags}$ | Number of air accumulators              | $w$       | Specific work                |
| $n$        | Number of compressor or expander stages | $z$       | Depth of air accumulator     |
| $P$        | Power                                   | $\beta$   | Pressure ratio               |
| $p$        | Pressure                                | $\beta_i$ | Stage pressure ratio         |
| $R$        | Gas constant                            | $\gamma$  | Specific heat ratio          |
| $T$        | Temperature                             | $\eta$    | Efficiency                   |

---

<sup>1</sup> This thesis incorporates the outcome of a joint research project undertaken in collaboration with Mr. Ning Cao under the supervision of Dr. Rupp Cariveau and Dr. David S-K. Ting. In all cases, the author performed the key ideas, primary contributions and data analysis and interpretation, and the contribution of the co-author was primarily through the provision of developing experimental designs and data collection.

<sup>2</sup> Corresponding author. Address: 401 Sunset Ave. Windsor, Ontario, Canada N9B 3P4. Telephone: 519-253-3000 ext. 2638. Email: rupp@uwindsor.ca

## **1.0 INTRODUCTION**

Today's energy landscape is laden with a growing deployment of many new technologies that are geared towards modernizing the present electricity system. Principal objectives of these technologies include improving: efficiency, reliability, resiliency and system sustainability. The largest growth sectors in the present energy industry include: the incorporation of renewable energy generators and the transformation of existing power grid into a smart grid.

The benefits of these two trends are significant – they help to make better use of existing electrical infrastructure, curb air emissions, and increase energy security, among many others. The shift towards greater use of renewable resources and smarter power grids is an essential step; however, the reality of the current conventional grid is that power generation remains a just-in-time process where electrical energy produced must be immediately consumed. The decoupling of the time of electricity production and consumption requires a major change in how electricity is managed. This can be accomplished through energy storage.

The aim of this paper is to examine the use of distensible air accumulators for use in underwater energy storage. An analysis of the concept is established and a general configuration of the equipment and processes used for energy storage underwater is discussed. Results of a pilot project that demonstrated field conditions of submerged air accumulators are analyzed.

### **1.1 The reason for energy storage**

Electrical energy storage (EES) is defined as a process in which electrical power is converted into chemical, mechanical, or electrical potential energy for the purpose of dispatching back into the power grid when needed [1]. Currently, it is of ever increasing



interest to the electricity market. Recent developments in energy prices, growing demand, pending major infrastructure renewal and significant use of intermittent generation sources like wind and solar have raised awareness of various EES technologies as a means of addressing current energy concerns. Storage has been recognized as a strategic tool in a modern grid [2].

To grid users and operators, the capacity to store large amounts of energy for consumption at a later time provides many advantages, including the reduction of power transmission and distribution congestion, efficient utilization of existing generation assets, improving power quality in the grid, and the potential of transforming intermittent generation supplies into dispatchable generation resources.

Since the storage of electricity itself is a difficult task, many current storage solutions convert the electrical power into a storable medium. The selection of a technology for energy storage can be based on the application and scale; existing technologies such as batteries, super magnetic energy storage, capacitors, and flywheels can be used for small-scale storage, whereas large-scale energy storage projects employ systems based on compressed air or pumped hydro [3].

## **1.2 Conventional Compressed Air Energy Storage**

Traditionally, compressed air energy storage (CAES) has been used as an alternative to pumped hydro storage for large-scale, bulk energy management. These CAES systems typically rely on electrically-driven air compressors that pump pressurized air into large underground geological formations such as aquifers and caverns for storage; at a later time, turbo-expanders connected to generators convert the compressed air back into electrical energy whenever the energy is needed. This process is shown in Figure 1.

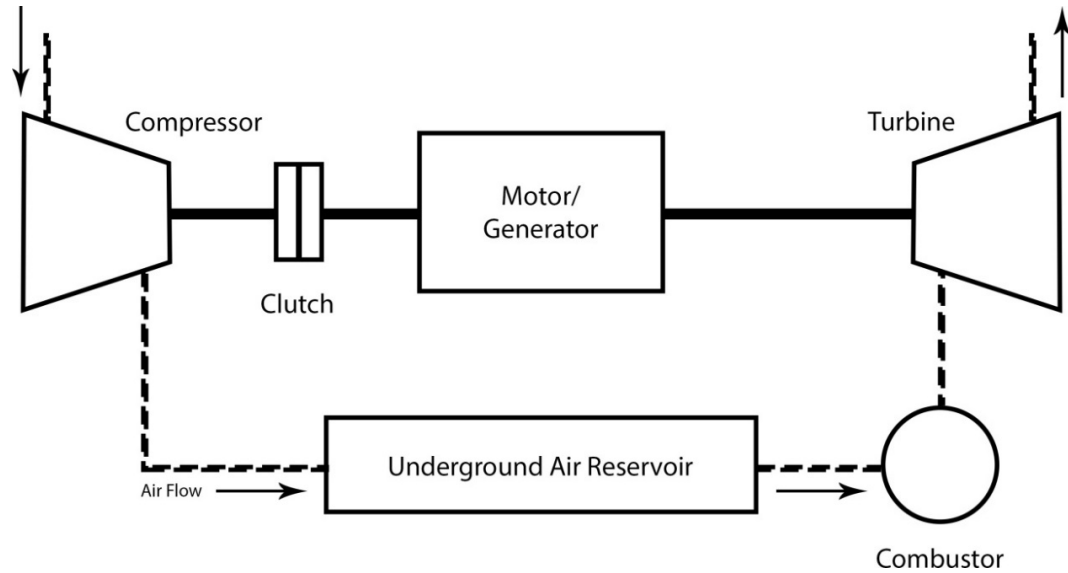


**Figure 1** - Traditional CAES process

The system lifetime, stored energy capacity per capital cost and output power per capital cost of CAES systems [4] make the technology an attractive means of energy storage amongst its competitors, especially when used for energy management [5]. The justification for the technology is particularly strong in places with favourable geologic and geographic conditions. Southwestern Ontario is such an example [6].

Due to the scale required for feasible plants, CAES technology has been reserved for bulk energy applications like energy arbitrage or support of base-load power plants. With the influx of renewable energy generation, it has been proposed for CAES technology to be extended to support large-scale renewable generation [7].

### **1.3 CAES technology in practice**

CAES has evolved throughout the last few decades since the 1970s when the technology was first proposed. Most of the developments in CAES technology deal with air preheating prior to air expansion. This is done primarily as a measure to prevent equipment damage, as the temperature of air cools down as it expands. In first generation CAES systems, combustors are used to heat the air entering expander

turbines. In second generation systems, air is preheated by exhaust from gas turbines [8]. With adiabatic CAES systems, the need for fuel is eliminated by employing a heat capture process that stores heat energy produced during air compression for use in preheating before air expansion [9].

Despite ongoing advancement of CAES designs over the years, to date, there are only two operating facilities constructed thus far; a 290 MW facility in Huntorf, Germany and a 110 MW installation in Alabama, USA. Both these plants are of the first generation design and have demonstrated strong performance – the Huntorf plant reported 90% availability and 99% starting reliability [10] while the McIntosh plant achieved 91.2% and 92.1% average starting reliabilities as well as 96.8% and 99.5% average running reliability for the generation cycle and compression cycle respectively over 10 years of operation [11]. Currently, new modern conventional-type CAES installations are undergoing planning and development, such as the ADELE project in Germany and the Norton Energy Storage Project in Ohio, to name a few. Early stage planning are underway in places like New York, Texas and California [12].

## **2.0 UNDERWATER COMPRESSED AIR ENERGY STORAGE**

CAES is a proven technology for effective bulk storage of energy. However, in a modern, smarter grid, cost-efficient and flexible scale storage solutions that can cater to both large and small scale applications are required. Underwater compressed air energy storage (UWCAES) is a promising solution that can fit that need.

UWCAES is an innovative variation of proven conventional CAES technology. Using mature technologies like air compression and expansion, UWCAES proposes the use of a series of submerged, distensible air accumulators as an alternative to large geological formations for the storage of compressed air, illustrated in Figure 2.

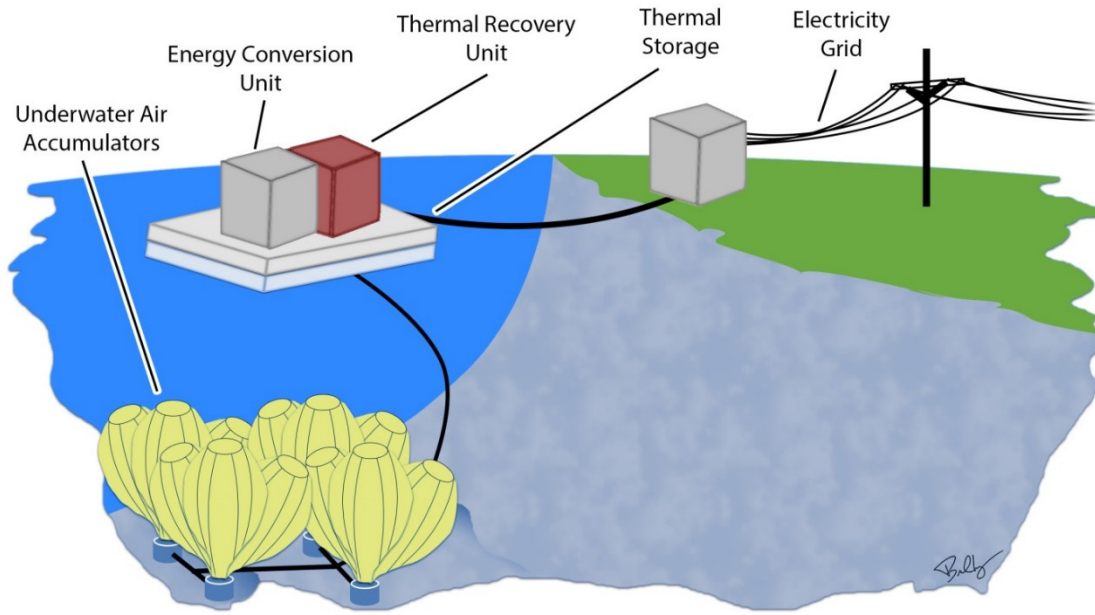


**Figure 2** - Illustration of a UWCAES system

Conceptually, the accumulators used in the UWCAES system are placed at or near the bed of deep water bodies such as lakes and oceans, utilizing the hydrostatic pressure exerted by the surrounding water. The extent of the accumulators will expand and contract depending on the amount of compressed air present within. Air compressed to a design pressure equal to the hydrostatic pressure at the accumulator storage depth would remain at constant pressure due to the environment, regardless of the accumulator's filled capacity.

In terms of the mechanical aspect of the system design, the setup is similar to that of adiabatic CAES. As air undergoes isentropic compression, its temperature rises; a highly effective thermal recovery process extracts energy from the hot air and stores it in a medium that features high specific heat capacity, high density, and good heat transfer characteristics. During isentropic air expansion, where compressed air is used to generate electricity, the stored energy is used to raise the temperature of the compressed air coming from the accumulators, prior to entering turbo-expansion equipment.

## **2.1 Benefits of UWCAES**

The distinct accumulator element in the UWCAES design provides important advantages compared to conventional systems; a practically constant energy output profile, geographical adaptability, and scalable design.

The energy output profile is dependent on the dynamics of the expanding air. In conventional CAES systems, the fixed volume capacity of the storage reservoir causes variability in air pressures as the mass of air stored changes. As air is being discharged, conventional systems will experience changing electrical output levels. This phenomenon does not occur in the UWCAES system; the accumulators maintain constant pressure through their distensible accumulators, even when partially filled with air. Near constant energy input and output is exhibited during charge and discharge phases of the system.

The placement of UWCAES plants is less restrictive than their conventionally terrestrial counterpart. With conventional CAES, specific geological conditions must be met when selecting sites. In a UWCAES installation, a deep body of water supplants the need for specialized geological sites, increasing flexibility in system placement. It is estimated that approximately half of the world's population is situated near a coastline [13]; UWCAES could be easily deployed near many population centers, foregoing the need for long distance transmission lines.

The application of a series of air accumulators to store compressed air affords a significant advantage in scalability. To increase the size of the reservoir in a UWCAES system is simply a matter of adding accumulators. This aspect is particularly useful for smaller-scale, distributed storage applications, where smaller reservoirs are needed.

## 2.2 UWCAES Configuration

The configuration of a UWCAES plant mirrors that of conventional adiabatic CAES; the system has five main components: compressor, turbines, motor/generator, air storage and the thermal recovery unit. Figure 3 depicts the general layout of the system.

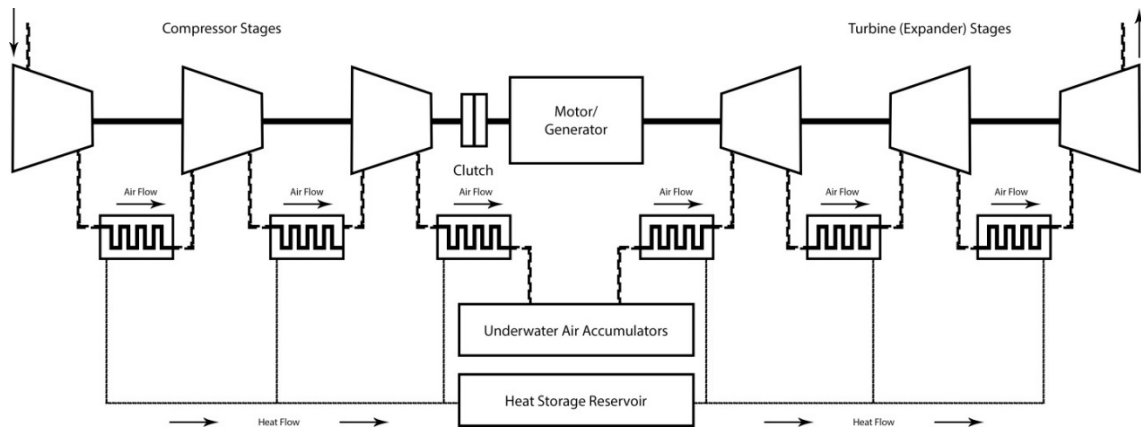


**Figure 3** - UWCAES system layout

For UWCAES, the depth at which the air accumulators are placed below the water surface governs the design storage pressure. The system is modelled using a three-stage polytropic compression/expansion process with intercooling, using ambient air as the working fluid. When the system is charging – energy being stored – a motor runs the multi-stage air compressor unit to pump pressurized air into the submerged air accumulators. After each compression stage, heat generated by the compression process is extracted from the air and stored by the thermal recovery unit (TRU) consisting of heat exchangers and a storage reservoir. During system discharge – where electricity is generated – air flows back through the TRU to be reheated prior to each expansion stage. The heated air is then sent through and expands in the turbines, which drives a generator to produce electricity.

### 2.2.1 Compressor/Turbine

Air is assumed to be an ideal gas, Eq. (1), and is compressed and expanded through a polytropic process, Eq. (2).

$$pv = RT \quad (1)$$

$$pv^\gamma = \text{const.} \quad (2)$$

Combining Eq. (1) and (2) will yield an isentropic relationship, as given in Eq. (3).

$$T_2 = T_1 (p_2 / p_1)^{\frac{\gamma-1}{\gamma}} = T_1 \beta^{\frac{\gamma-1}{\gamma}} \quad (3)$$

As the UWCAES system uses multi-stage compression and expansion, optimum work by the machinery is achieved by maintaining equivalent pressure ratios across all  $n$  stages. The stage pressure ratio  $\beta_i$  is found through Eq. (4)

$$\beta_i = (p_f / p_i)^{1/n} \quad (4)$$

The specific work for an isentropic process, based on the first law of thermodynamics, is given in Eq. (5).

$$w = \int v \, dp \quad (5)$$

Combining Eq. (3) into Eq. (5) results in an expression to determine the specific work for an individual compression or expansion stage, indicated in Eq. (6).

$$w = \frac{\gamma}{\gamma-1} RT_1 \left( \beta_i^{\frac{\gamma-1}{\gamma}} - 1 \right) \quad (6)$$

In practice, inefficiencies are present whenever work is done; the isentropic efficiency is assigned to the compressors and expanders, which is calculated by Eq. (7) and (8).

$$\eta_{comp} = \frac{w_{ideal}}{w_{actual}} \approx \frac{T_{2,s} - T_1}{T_{2,a} - T_1} \quad (7)$$

$$\eta_{exp} = \frac{w_{actual}}{w_{ideal}} \approx \frac{T_1 - T_{2,a}}{T_1 - T_{2,s}} \quad (8)$$

### 2.2.2 Motor/Generator

For multi-stage air compression, a compressor-train is used and driven by an electric motor. In multi-stage air expansion, a turbine-train is connected to a shaft and drives a generator, producing an electrical output. Considering the mechanical losses of individual devices, the actual input shaft power to the compressor, and the power rating of the expander are estimated using Eq. (9) and (10).

$$P_{comp,a} = \frac{P_{shaft}}{\eta_{mech}\eta_{comp}} \quad (9)$$

$$P_{exp,a} = \eta_{mech}\eta_{exp}P_{shaft} \quad (10)$$

An important performance measure of energy storage systems is its round trip efficiency. Unlike regular CAES systems, where external sources of energy are used to heat up the air, the overall system efficiency is determined using Eq. (11).

$$\eta_{round-trip} = E_{out} / E_{in} \quad (11)$$

In practice, it is generally expected that an adiabatic CAES system is able to achieve a round trip efficiency of 70%. Based on a thermodynamic analysis by Grazzini and Milazzo [14], a system could potentially have an efficiency of close to 72%.

### 2.2.3 Underwater Air Storage

In the case of UWCAES, the underwater air accumulators used must be adequately designed to be able to withstand the environment they are placed in. As well,



care needs to be taken when anchoring the accumulators to the bedding of deep water bodies.

The UWCAES design uses a series of smaller, submerged accumulators. These accumulators borrow many concepts from underwater lift and salvage balloons. As mentioned earlier, air inside the accumulators maintains constant pressure during storage and near constant pressure during system charge and discharge. This allows for more consistency in power output.

The number of accumulators required for air storage is dependant the depth of storage and the corresponding air pressure, the mass of air stored, and the design accumulator volume. This relationship is indicated in Eq. (13). Generally, the deeper the accumulators are placed in the water, the lower the number of accumulators will be.

$$N_{bags} = f(z, p_{air}, m_{air}, V_{bag}) \quad (13)$$

Since a series of accumulators are used to store air, an air distribution network of pipes is needed to direct the flow of air from the compressor/expander equipment to the accumulators, and vice versa. Potential pressure losses must be taken into careful consideration when developing the pipe network; a constraint with more significance to UWCAES compared to other CAES systems.

Different concepts have been proposed in storing compressed air underwater. As an example, a survey of alternative accumulator designs has resulted in a proposal by Pimm and Garvey [15], in which large fabric structures with a diameter in the order of 20 meters were analyzed.

#### 2.2.4 Thermal Recovery

An effective thermal recovery process is crucial to the operation of a UWCAES system. In addition to electrical energy storage, the UWCAES features thermal energy

storage; two forms of energy are stored. Since heat is needed to bring up the temperature of the air coming from the accumulator prior to entering the turbines for expansion, sufficient thermal energy must be captured, transferred and stored. When designing the TRU, a suitable storage medium and temperature must be determined, and proper heat exchangers selected. The TRU should be designed to minimize the amount of heat lost to the surrounding for extended durations of storage.

The science of thermal recovery is quite mature. Resources such as Chapter 34 of [16] should be consulted regarding thermal recovery design.

### **3.0 UWCAES PILOT PROJECT**

#### **3.1 Experimentation**

A pilot project evaluating the distensible air accumulator aspect of the UWCAES concept was completed; this project did not study the mechanical and thermodynamic aspects of the UWCAES system. Representative mechanical and thermodynamic analyses can be found in [14], [17], [18], as UWCAES is similar to that of conventional adiabatic CAES systems.

In the pilot project test, a modified 1:5 scale lift bag was utilized as the accumulator. Figure 4 shows the experimental configuration. The accumulator was anchored on two 9 tonne concrete cylinders. A feeder hose with a diameter of 20 mm was connected to the top of the accumulator to facilitate charging and discharging phases of the system. Several pressure safety valves were attached to the bottom of the accumulator to ensure safe operational pressure. A 25 mm diameter hose connected the test accumulator to a compressor situated on shore.

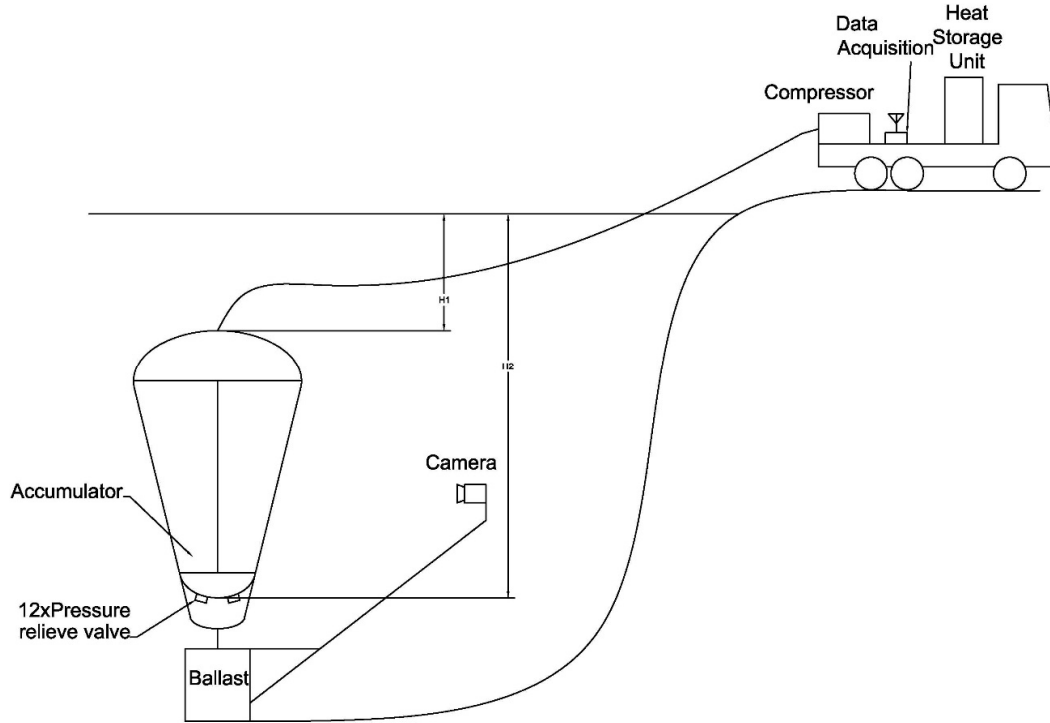


**Figure 4** - Experimental configuration of pilot project

The experiment for the accumulator was conducted in two phases; first, the discharge cycle, where air is released from the accumulator, then second, the charge cycle, where air is pumped into the accumulator by the compressor. Using a series of pressure and temperature sensors, flow meters and data acquisition equipment, results were collected.

## 3.2 Results

### 3.2.1 Accumulator Discharging Phase

The accumulator was first discharged at an initial pressure of 195 kPa. Figure 5 shows the pressure and flow data of the discharge phase. A sharp decrease in the temperature and pressure and increase in flow rate was observed at the very beginning of the discharge period that lasted less than a minute. After five time constants from the start of the discharge period, corresponding to the values measured at 113 seconds, the

system discharge began to stabilize at a pressure of 134 kPa and a flow rate of approximately 0.005 kg/s. An initial pressure loss of approximately 61 kPa can be seen at this point; this is attributed to friction and minor losses due to the pipe configuration. This was verified using the Bernoulli equation.

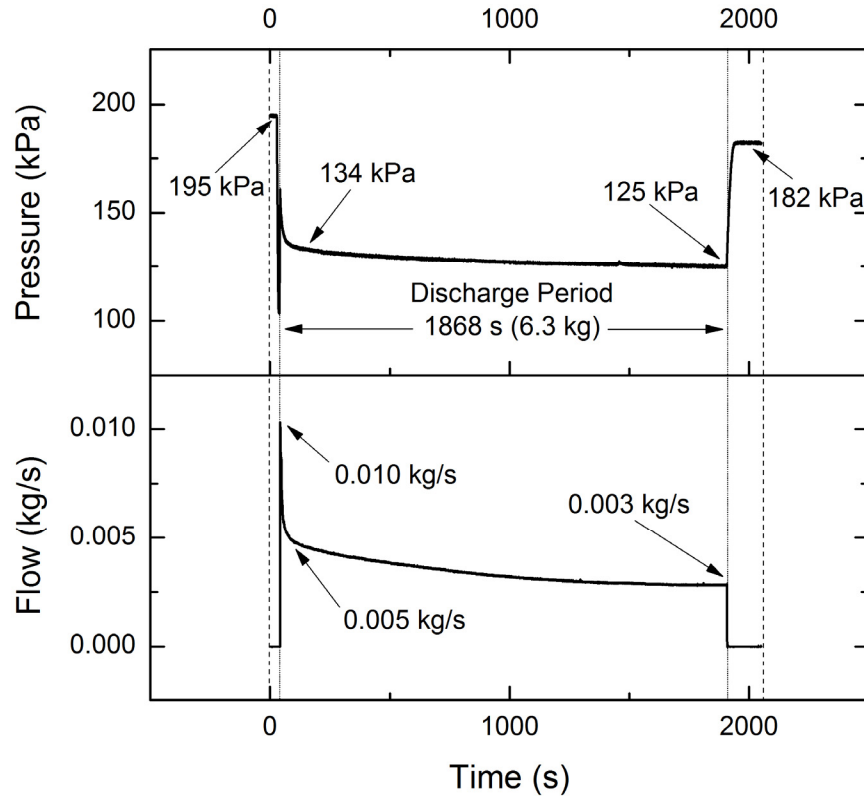


**Figure 5** - Accumulator discharge data

From the cycles performed, the average discharge period of a cycle lasted around 30 minutes. When analyzing the 1868 second discharge cycle, 6.3 kg of air was removed from the accumulator. During discharge, the pressure reduced from 134 kPa to 125 kPa. As well, the mass flow rate decreased from 0.005 kg/s to 0.003 kg/s. Once the air flow was shut off, the final pressure in the accumulator stabilized to 182 kPa. The removal of 6.3 kg of air resulted in a pressure drop of 13 kPa in the accumulator.

### 3.2.2 Accumulator Charging Phase

The air flow rate during the accumulator charging was higher than the discharge phase due to the compressor that was used – it operated at a minimum charging rate of 0.023 kg/s. As such, tests for this phase were relatively short; based on the flow rate, full accumulator charging took roughly 3 minutes.

Data for the accumulator charging cycle is shown in Figure 6. Initial air pressure in the accumulator was 182 kPa. Once the charging process began, air was delivered to the accumulator at a rate of 0.0252 kg/s. After 246 seconds, a total of 5.7 kg of air was added back into the accumulator, and pressure returned to 195 kPa. As air pressure was measured on the compressor side of the piping, the high flow rate of air through a narrow pipe diameter resulted in significant pressure loss, causing an air compressor's discharge pressure of 730 kPa.

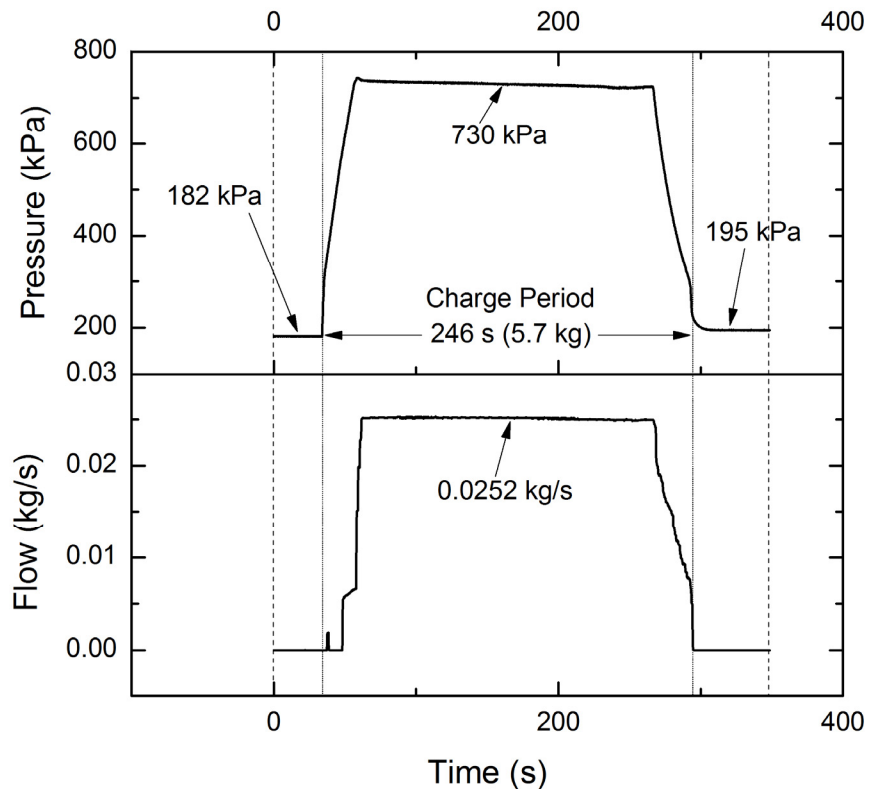


**Figure 6** - Accumulator charge data

### 3.3 Discussion

The pilot project showed that some variation in flow rates and pressures occur during the cycling of air in the accumulator, especially during the discharge phase; the charging phase maintained consistently predictable performance during system operation. While the variations do occur, the general behaviour of the processes remains predictable. When designing the full scale UWCAES system, they can be controlled and mitigated using carefully developed strategies.

Ideally, when the accumulator discharges, constant air pressure is maintained. However, as shown in the discharge phase results of the pilot project, a slight pressure drop occurs from beginning and end of cycle. The root cause of this pressure drop may be attributed to the vertical hydrostatic pressure difference between the top and bottom of the accumulator. As air leaves the top of the accumulator, the larger pressure at the bottom is pushed upwards, decreasing the overall pressure of the bag (the contained volume is at a lower pressure). As the pressure decreases, so too does the flow rate.

When examining the flow rate from Figure 5, a noticeable spike of 0.010 kg/s exists. This corresponded to the opening of a valve to release the air. While the vertical pressure difference has a major effect on the flow rate, an additional factor can be considered; the accumulator itself. A fully charged accumulator would have an internal pressure equal to the hydrostatic pressure at the bottom of the bag. As such, a pressure difference between the compressed air and the surrounding water exists at the accumulator top; this would imply that the stresses at the top of the accumulator are balanced by the tension in the accumulator material. When air depletes, this pressure difference will reduce, lowering the air flow rate. These pressure and flow effects are functions of the accumulator geometry particular to this experiment. For instance, results for horizontally oriented, cylindrical accumulators would prove different.

## **4.0 CONCLUSIONS**

The potential for UWCAES as a means for cost-efficient and flexible energy storage in the modern electricity industry has been examined. By using submerged, distensible air accumulators for energy storage, UWCAES systems have the potential to be implemented in strategic locations at various scales to enhance the power grid.

An analysis of the pilot project demonstrating the charge and discharge cycles of the balloon shaped air accumulator showed that it may be representative of a potentially feasible alternative to the large underground reservoirs of conventional CAES systems. The operation of the accumulator is predictable and with further improvements in the design of the pipe distribution network and accumulator design, performance can be improved over those results presented here.

## **ACKNOWLEDGEMENTS**

The research and development of the UWCAES system is in partnership with Hydrostor Inc., with funding from the Ontario Centres of Excellence and Sustainable Development Technology Canada.

## **REFERENCES**

- [1] R. Baxter, *Energy Storage - A Nontechnical Guide*. PennWell, 2007.
- [2] Electricity Advisory Committee, “Bottling Electricity: Storage as a Strategic Tool for Managing Variability and Capacity Concerns in the Modern Grid,” Dec. 2008.
- [3] F. Díaz-González, A. Sumper, O. Gomis-Bellmunt, and R. Villafáfila-Robles, “A review of energy storage technologies for wind power applications,” *Renewable and Sustainable Energy Reviews*, vol. 16, no. 4, pp. 2154–2171, May 2012.
- [4] J. Kondoh, I. Ishii, H. Yamaguchi, A. Murata, K. Otani, K. Sakuta, N. Higuchi, S. Sekine, and M. Kamimoto, “Electrical energy storage systems for energy networks,” *Energy Conversion and Management*, vol. 41, no. 17, pp. 1863–1874, Nov. 2000.

- [5] H. Chen, T. N. Cong, W. Yang, C. Tan, Y. Li, and Y. Ding, "Progress in electrical energy storage system: A critical review," *Progress in Natural Science*, vol. 19, no. 3, pp. 291–312, Mar. 2009.
- [6] J. Konrad, R. Cariveau, M. Davison, F. Simpson, and D. S.-K. Ting, "Geological compressed air energy storage as an enabling technology for renewable energy in Ontario, Canada," *International Journal of Environmental Studies*, vol. 69, no. 2, pp. 350–359, 2012.
- [7] J. E. Mason and C. L. Archer, "Baseload electricity from wind via compressed air energy storage (CAES)," *Renewable and Sustainable Energy Reviews*, vol. 16, no. 2, pp. 1099–1109, Feb. 2012.
- [8] M. Nakhamkin, M. Chiruvolu, M. Patel, S. Byrd, R. Schainker, and J. Marean, "Second Generation of CAES Technology- Performance, Operations, Economics, Renewable Load Management, Green Energy," presented at the POWER-GEN International, Las Vegas Convention Center, Las Vegas, NV, 2009.
- [9] S. Zunft, C. Jakiel, M. Koller, and C. Bullough, "Adiabatic compressed air energy storage for the grid integration of wind power," presented at the Sixth Edition, International Workshop on Large-Scale Integration of Wind Power and Transmission Networks for Offshore Windfarms, 26-28 October 2006, Delft, the Netherlands, 2006, pp. 346–351.
- [10] F. Crotogino, K.-U. Mohmeyer, and R. Scharf, "Huntorf CAES: more than 20 years of successful operation," in *Solution Mining Research Institute Meeting, Orlando, FL*, Orlando, FL, 2001.
- [11] L. Davis and R. Schainker, "Compressed Air Energy Storage (CAES): Alabama Electric Cooperative McIntosh Plant - Overview and Operational History," presented at the Electricity Storage Association Meeting 2006: Energy Storage in Action, Knoxville, Tennessee, 2006.
- [12] S. Succar and R. Williams, "Compressed Air Energy Storage: Theory, Resources and Applications for Wind Power," Princeton University Energy Systems Analysis Group, 2008.
- [13] L. Creel, "Ripple Effects: Population and Coastal Regions," Population Reference Bureau, 2003.
- [14] G. Grazzini, "Thermodynamic analysis of CAES/TES systems for renewable energy plants," *Renewable Energy*, vol. 33, no. 9, pp. 1998–2006.
- [15] A. Pimm and S. Garvey, "Analysis of flexible fabric structures for large-scale subsea compressed air energy storage," *Journal of Physics: Conference Series*, vol. 181, p. 012049, Aug. 2009.



- [16] American Society of Heating, Refrigerating and Air-Conditioning Engineers, Inc., *2007 ASHRAE Handbook - Heating, Ventilating, and Air-Conditioning Applications*, I-P ed. 2007.
- [17] G. Grazzini and A. Milazzo, "A Thermodynamic Analysis of Multistage Adiabatic CAES," *Proceedings of the IEEE*, vol. 100, no. 2, pp. 461–472, Feb. 2012.
- [18] N. Hartmann, O. Vöhringer, C. Kruck, and L. Eltrop, "Simulation and analysis of different adiabatic Compressed Air Energy Storage plant configurations," *Applied Energy*, vol. 93, pp. 541–548, May 2012.

## CHAPTER III

# PARAMETERS AFFECTING SCALABLE UNDERWATER COMPRESSED AIR ENERGY STORAGE

BRIAN C. CHEUNG, RUPP CARRIVEAU<sup>1</sup>, DAVID S-K. TING

Turbulence and Energy Laboratory, Ed Lumley Centre for Engineering Innovation,  
University of Windsor, Ontario, Canada, N9B 3P4

Under review for publication in the journal “Applied Energy”

## NOMENCLATURE

|       |   |                   |                                     |
|-------|---|-------------------|-------------------------------------|
| $c_p$ | Constant pressure specific heat, kJ/kg·K              | $u$               | Specific internal energy, kJ/kg     |
| $c_v$ | Constant volume specific heat, kJ/kg·K                | $\bar{V}$         | Velocity, m/s                       |
| $D$   | Pipe diameter, m                                      | $V$               | Volume, m <sup>3</sup>              |
| $f$   | Darcy's friction factor                               | $v$               | Specific volume, m <sup>3</sup> /kg |
| $g$   | Gravitational acceleration constant, m/s <sup>2</sup> | $w$               | Specific work, kJ/kg                |
| $K_L$ | Minor loss coefficient                                | $X$               | Exergy, kJ                          |
| $k$   | Specific heat ratio                                   | $X_D$             | Exergy destruction, kJ              |
| $L$   | Pipe length, m  | $x$               | Specific exergy, kJ/kg              |
| $m$   | Mass, kg  | $z$               | Accumulator depth, m                |
| $N$   | Number of compressor/turbine stages                   |                   |                                     |
| $n$   | Polytropic exponent                                   | <b>Greek</b>      |                                     |
| $P$   | Power, kW   | $\beta_i$         | Stage pressure ratio                |
| $p$   | Pressure, kPa   | $\varepsilon$     | Pipe roughness, m                   |
| $p_L$ | Pressure loss, kPa                                    | $\eta$            | Efficiency                          |
| $R$   | Universal gas constant, kJ/kg·K                       | $\rho$            | Density, kg/m <sup>3</sup>          |
| $Re$  | Reynolds number                                       |                   |                                     |
| $s$   | Specific entropy, kJ/kg·K                             | <b>Subscripts</b> |                                     |
| $T$   | Temperature, K  | 0                 | at reference condition              |
| $t$   | Time, s   |                   |                                     |

---

<sup>1</sup> Corresponding author. Tel: +1 519 253 3000. Email address: rupp@uwindsor.ca

## **1.0 INTRODUCTION**

Electrical energy storage (EES) is an increasingly important element to the modernization of the electrical grid. Traditionally, the aging infrastructure currently in place handled stable electricity production from large, centralized plants. With the advent of wide-scale deployment of renewable energy generation from wind and solar, electricity distribution networks are required to incorporate energy sourced from smaller, naturally intermittent distributed generation, while ensuring power reliability. Various technologies and policies have technological been proposed for integrating renewable energy sources (RES) [1], with EES gaining traction as a critical solution for reliable RES integration [2-6]. As well, EES has been recognized for the services and benefits it provides to electricity grid operation [7,8].

EES is a set of technologies that decouples electricity production and demand, by allowing the flexible storage of power for later use [9]. As electricity itself cannot be stockpiled in large quantities, EES systems convert the electrical power into a storable medium that includes chemical, mechanical and electrical potential energies. When power is needed, the stored energy is converted back into electricity and is injected into the electrical grid. One such technology gaining interest is compressed air energy storage (CAES).

CAES is a storage technology that utilizes a series of air compressors to pressurize and store ambient air in reservoirs. The compressed air is converted back to electricity by generator-coupled air expanders. In applications to date, CAES systems have been applied at large, utility scales (>100 MW) for bulk energy storage. It has often been considered as an alternative to pumped hydro storage (PHS) for large-scale storage [10], primarily for its low energy costs due to its inexpensive storage media and its large storage capacity [11,12].

This paper examines a novel adaptation of CAES technology known as underwater compressed air energy storage (UWCAES), where submerged, distensible air accumulators are used to facilitate energy storage. The accumulators used in the system offer two important design characteristics – a scalable design and isobaric system charge and discharge profiles. These characteristics address some limitations of conventional CAES systems pertaining to the storage reservoir, that is, the geology-restricted system capacity [3,6] and capacity-linked storage pressure variation [13]. This study presents an energy and exergy analysis of an UWCAES system in order to understand the impact design parameters may have on the system’s overall performance. As well, a sensitivity analysis is performed to determine a hierarchy of influential system variables. The findings of this paper can serve as an initial guideline for the design of future UWCAES systems.

## **2.0 UNDERWATER COMPRESSED AIR ENERGY STORAGE**

The UWCAES system builds on established concepts proven by reliable installations in Huntorf, Germany [14] and McIntosh, Alabama, USA [15], to bring CAES applications to smaller scales while eliminating fossil fuel use. It is similar to that of the adiabatic CAES concept, in which thermal energy storage is used to replace the combustion chamber of a CAES system [16]. The basic process architecture of an UWCAES system is given in Figure 1. A general UWCAES system consists of five main components: compressor, turbine, motor/generator, thermal recovery unit (TRU) and storage (air and thermal). The air storage is made up of a series of air accumulators, all of which are connected to an air delivery pipe network. Figure 2 and 3 depicts two possible configurations of an UWCAES system. During the system charge phase where energy is stored, ambient air is compressed and sent to the air accumulators. Heat generated during the compression process is extracted from the air by the TRU – a series of heat

exchangers (HEX) – and stored in a suitable thermal storage medium. In the case of discharging, the air is first released from storage, heated up by the TRU and expanded through a turbine. A generator is connected to the turbine to produce an electrical output.

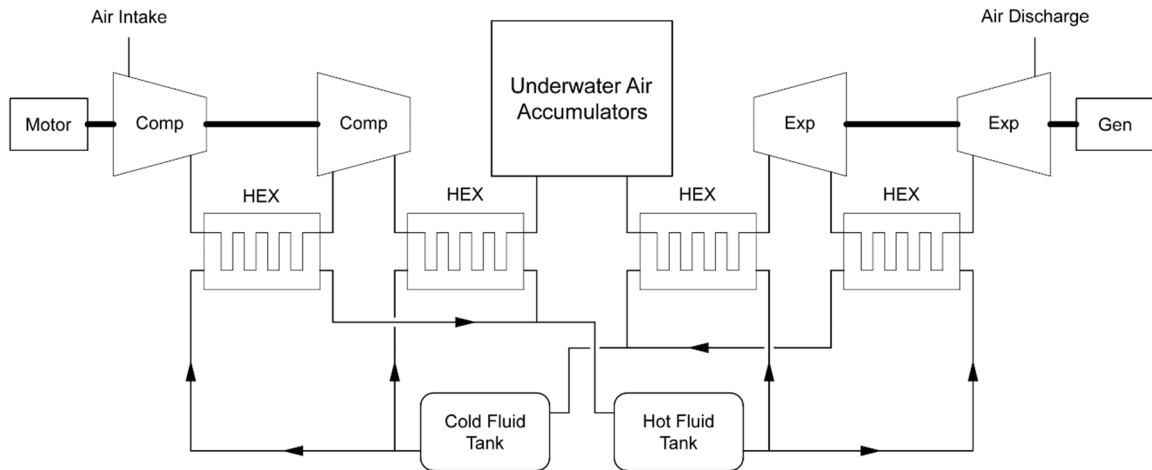


**Figure 1** – UWCAES process diagram

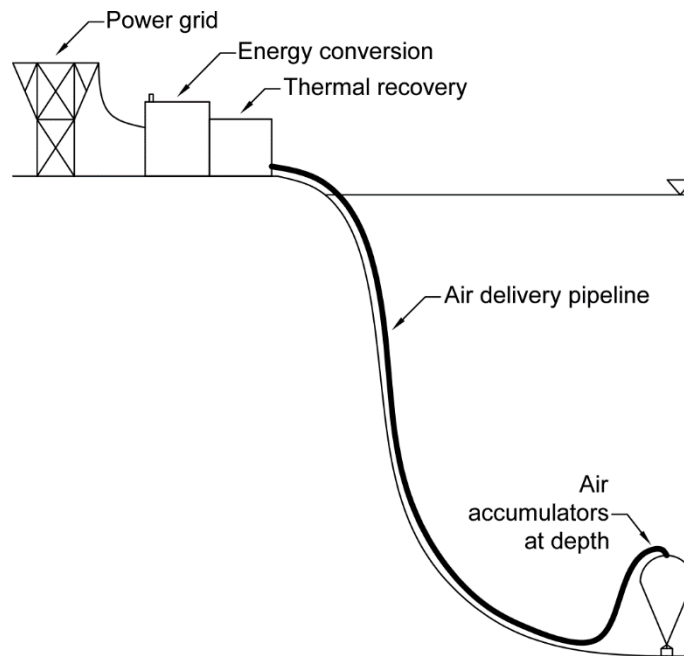


**Figure 2** – A land-based UWCAES system

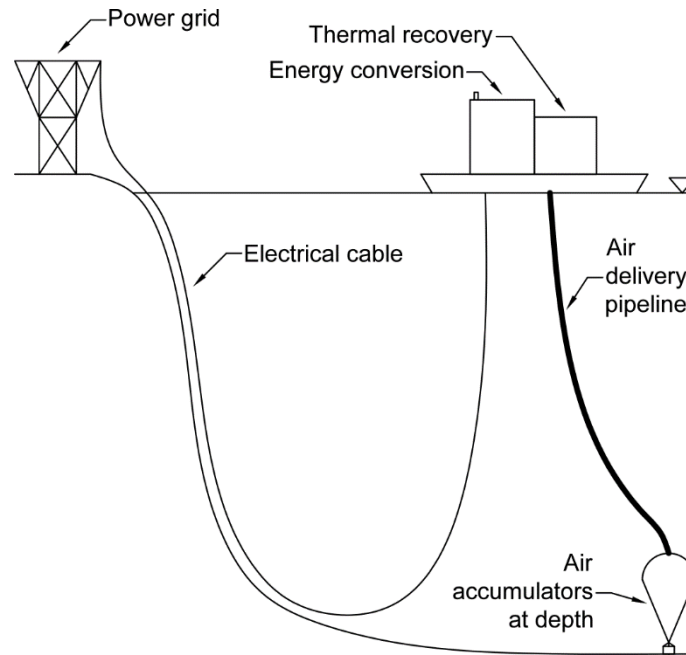


**Figure 3** – An UWCAES system located on an off-shore barge

The storage reservoir is a critical element for consideration when designing and siting a CAES system. The application of submerged, distensible air accumulators is the UWCAES system's defining aspect. Traditional CAES has relied on locations with suitable geologic formations, demonstrated in the world's two operating CAES plants – a 290 MW plant in Huntorf, Germany and a 110 MW plant in McIntosh, Alabama, USA – both using large underground, solution-mined salt caverns [12]. Such fixed reservoirs are rigid in nature; CAES systems operate under constant volume conditions and experience variable pressures based on its filled capacity. In the UWCAES solution, the air accumulators are anchored to the bedding of lakes or oceans and rely on the hydrostatic pressure exerted by the surrounding water at depths to maintain the stored air pressure. The flow of air entering and leaving the air accumulators exhibit a near-isobaric behaviour regardless of the accumulator's filled capacity [17].

The constant pressure condition in CAES is desirable as it leads to increased efficiency in the pneumatic equipment, specifically the turbine, as well as constant power

profiles. The two existing CAES facilities have pursued this aspect by throttling air flow at the turbine inlet to maintain a high pressure [13]. When system efficiency is paramount, this method can lead to unwanted losses. As such, a couple of alternate solutions to achieve isobaric performance in land-based CAES systems have been presented. In [18], a water-compensated CAES system using a water head supplied by an aboveground water reservoir is analyzed. Air pressure in the storage cavern is maintained by a water column or hydraulic pump; the choice depends on the depth of the cavern below surface. It should be noted that a water-compensated CAES system can only be applied to certain storage reservoirs; for example, a salt cavern air reservoir is unsuitable for this configuration. A unique CAES concept was proposed in [19], where constant pressure airflow is achieved by storing compressed air in nano-porous material.

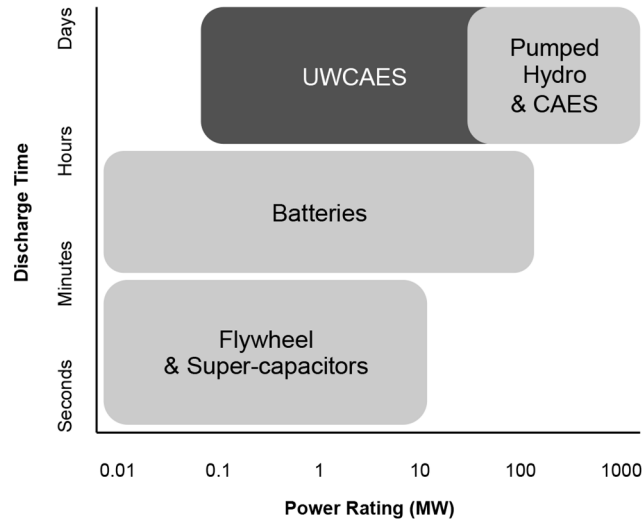


**Figure 4** – UWCAES among other EES technologies

In terms of storage capacity, the UWCAES air reservoir can be scaled by the addition or subtraction of accumulator units. This allows for CAES applications at scales normally impractical for geologic CAES. Figure 4 shows UWCAES with respect to other energy storage technologies. However, there have been other investigations for small-

scale CAES. In [20], an analysis of a micro-CAES system using man-made air vessels was performed. Quasi-isothermal and adiabatic configurations of a water-compensated constant pressure micro-CAES were evaluated. Also using pressure tanks [21], a hybrid wind-diesel system combined with CAES for application in remote regions was explored. Guidelines for pressure vessel sizing for small-scale CAES systems were presented in [22]. The study examined a stress analysis model for different vessel volumes subjected to various pressures, and provided an approximate equation for determining the pressure associated with the minimum vessel cost. Aside from pressure vessels, the feasibility of steel pipe piles for small-scale CAES was studied in [23].

Few researchers have explored the underwater CAES adaptation thus far. In [24], the concept of an ocean compressed air energy storage was discussed. In this system, a receiver vessel, vented to seawater, is mounted on the sea floor at depths in the order of 300-700 m. Compressed air moving in and out of the vessel displaces seawater. In [25], the shape of a large ‘energy bag’ was proposed and optimized to store compressed air at significant depths. The energy bag concept was further studied in [26], where a prototype bag with a meridional length of 2.36 m was modelled to analyze its shape and cost, particularly when deformed. A field study of an underwater lift bag-based air accumulator was presented in [27] demonstrating the near-isobaric behaviour of the air accumulator.

### **3.0 SYSTEM MODELLING**

#### **3.1 Design Theory**

The design pressure of an UWCAES system is dictated by the submergence of the air accumulators. It is determined by the hydrostatic pressure exerted by water at depth, given in equation (1).



$$p_{storage} = p_{atm} + \rho_{water} g z \quad (1)$$

In conventional CAES with rigid air storage reservoirs, designed storage pressures have been known to be upwards of 70 bar [28]. On the contrary, UWCAES systems tend to operate at lower pressures. While the high pressures of conventional CAES systems could be achieved by UWCAES at the appropriate depths, it may prove cost prohibitive and unnecessary for small-scale energy storage.

Taking the storage reservoir as the control volume, the mass of air can be calculated using the ideal gas law, shown in equation (2), given that the flow of air in the system is an isobaric process and that air behaves as an ideal gas at low temperatures and pressures. While in storage, air reaches thermal equilibrium with the water temperature at depth.

$$m_{air} = \frac{(pV)_{storage}}{RT_{water}} \quad (2)$$

### 3.1.1 Air Compression and Expansion

Multistage configurations are typically used to handle large pressure changes during air compression and expansion. If all stages in an air compressor or turbine are identical, the pressure ratio for each stage can be expressed by equation (3).

$$\beta_i = (p_{discharge} / p_{inlet})^{1/N} \quad (3)$$

Combining the ideal gas law and the polytropic process equation, given in equation (4), the outlet temperature of an air compression or expansion stage can be expressed as a function of pressure ratio, expressed as equation (5).

$$pv^n = const. \quad (4)$$

$$T_2 = T_1 \beta_i^{(n-1)/n} \quad (5)$$

If the isentropic efficiency is known, the polytropic exponent can be calculated using equation (6). For this study, the values of isentropic efficiency were sourced from manufacturer data.

$$n = \left[ 1 - \frac{1}{\log \beta_i} \log \left( 1 + \frac{1}{\eta_{isentropic}} (\beta_i^{(k-1)/k} - 1) \right) \right]^{-1} \quad (6)$$

The specific heat ratio,  $k$ , is calculated using equation (7). Its typical value for air is 1.4.

$$k = c_p / c_v \quad (7)$$

The specific work for a steady flow, polytropic device is given in equation (8).

$$w = \int_1^2 v \, dp = \frac{nR(T_2 - T_1)}{n-1} = \frac{nRT_1}{n-1} (\beta_i^{(n-1)/n} - 1) \quad (8)$$

The operational charge and discharge times can be determined using equation (9) for different power requirements.

$$t = \frac{m_{air} w}{P} \quad (9)$$

### 3.1.2 Thermal Recovery

Effective thermal management is a crucial element in a CAES system. Comprising of HEXs and thermal storage reservoirs, the TRU serves to enhance performance and protect air compression and expansion equipment while eliminating the need for heating using fossil fuels. The lower temperatures experienced in UWCAES air compression and expansion provides design flexibility. As an example, thermal recovery can be achieved by an open loop system using lake water as the thermal storage medium.

The design of HEXs is central to effective thermal recovery. They must be adequately sized to ensure optimal heat extraction during air compression and heat addition during air expansion. Different design methods for HEX sizing and performance evaluation are available and can be found in design handbooks [29].

### 3.1.3 Air Delivery Pipe Network Design

The UWCAES system's novel air storage reservoir requires properly sized pipes and fittings to minimize pressure losses associated with friction (major) or bends (minor). The calculation for pressure loss is given in equation (10), with the  $f$  estimated using the Moody chart [30, p. 898] or equation (11). The coefficients of  $K_L$  for different pipe fittings can be determined from various design resources.

$$p_L = p_{L,major} + p_{L,minor} = \left( f \frac{L}{D} + \sum K_L \right) \frac{\rho \bar{V}_{avg}^2}{2} \quad (10)$$

$$\frac{1}{\sqrt{f}} = -2.0 \log \left( \frac{\epsilon/D}{3.7} + \frac{2.51}{\text{Re} \sqrt{f}} \right) \quad (11)$$

## 3.2 Configuration

A numerical model was developed to simulate a single charge-discharge cycle a conceptual UWCAES system and its components. It was assumed that the simulated system was installed in a fresh water lake. The layout of the system mirrors the setup depicted in Figure 2, where mechanical and electrical components are situated on-shore and connected to the air accumulators through an air delivery pipeline.

### 3.2.1 Air Compression and Expansion

The system under consideration featured three air compression stages and three air expansion stages. During air compression, the first stage inlet temperature was set to the ambient air temperature. Trailing stages had a set inlet temperature of 12°C. Each

stage had an identical pressure ratio. The discharge pressure of the compressor was adjusted for pipe pressure losses. It was assumed that the power input into the three-stage compressor was 950 kW, after accounting for a motor efficiency 95%.

During air expansion, the inlet temperature of each turbine stage was determined following a performance evaluation on the HEX units. Identical pressure ratios were maintained across all three expansion stages. A generator efficiency of 97% was applied to the expander power output.

### *3.2.2 Thermal Recovery*

A set of three flat-plate, counter-flow HEXs were evaluated in the UWCAES system. The HEXs were sized according to temperature requirements during air compression. The sizing was based on number of stainless steel plates, with each plate having a dimension of 1.5m x 2 m and a thickness of 0.75 mm. A 4 mm gap between plates was assumed. A 60% ethylene glycol solution was used as the thermal storage medium. The HEX units were applied in reverse order during air expansion. The outlet temperature and pressure of each HEX was obtained through performance evaluation.

Ethylene glycol, heated up from ambient temperature during air compression, was stored in a vertical cylindrical tank with a diameter of 6 m, insulated using aerogel with a thermal conductivity of 0.021 W/m·K. An 8 hour gap between system charge and discharge phases was assumed. The temperature drop in the ethylene glycol during storage was calculated for every 15 minute interval.

### *3.2.3 Piping and Air Storage*

The model used a single HDPE header pipe, with a roughness of 0.003 mm, to connect the air accumulators to the equipment. Each accumulator, with a storage volume of 50 m<sup>3</sup>, was individually connected to the header pipe. The minor losses associated

with pipe fittings were assumed to be negligible. The length of the header pipe was calculated as a function of the accumulator's offshore distance and depth.

### 3.3 Methodology

A parametric study was conducted on the system model at different design points. Table 1 summarizes the system analysis baseline. Table 2 lists the design parameters under study and their variations. For each design case, the round-trip efficiency was evaluated and an exergy analysis was performed. The subject of interest in the exergy analysis was its destruction. Following the parametric study, a first-order sensitivity analysis was performed on the simulation results to determine the total impact each design parameter had on round-trip efficiency and exergy destruction. Subsequently, each parameter was ranked according to its effect in improving system performance.

**Table 1** – Baseline values

| <b>Variable</b>                             | <b>Baseline Value</b> |
|---|-----------------------|
| Reference environment (ambient) temperature | 8°C                   |
| Reference environment (ambient) pressure    | 101.325 kPa           |
| System output                               | 4000 kWh              |
| Accumulator depth                           | 100 m                 |
| Off-shore distance                          | 5000 m                |
| Number of compression/expansion stages      | 3 stages each         |
| System power input                          | 1000 kW               |
| Compressor isentropic efficiency            | 80%                   |
| Compressor motor efficiency                 | 95%                   |
| Maximum HEX extraction temperature ratio    | 0.8                   |
| Heat storage insulation thickness           | 10 mm                 |
| Header pipe diameter                        | 350 mm                |
| Expander isentropic efficiency              | 80%                   |
| Expander generator efficiency               | 97%                   |
| Charge-discharge time ratio                 | 2                     |

**Table 2** - Parameter variation

| Design Parameter                             | Variation | Range       |
|--|-----------|-------------|
| (1) Air storage depth                        | ±50%      | 50-150 m    |
| (2) Off-shore distance                       | ±50%      | 2500-7500 m |
| (3) System power input                       | ±50%      | 500-1500 kW |
| (4) Compressor isentropic efficiency         | ±12.5%    | 70-90%      |
| (5) Maximum HEX extraction temperature ratio | ±12.5%    | 0.7-0.9     |
| (6) Heat storage insulation thickness        | ±50%      | 5-15 mm     |
| (7) Header pipe diameter                     | ±50%      | 175-525 mm  |
| (8) Expander isentropic efficiency           | ±12.5%    | 70-90%      |
| (9) Charge-discharge time ratio              | ±50%      | 1-3         |

The round-trip efficiency of the system is a widely used term when comparing EES systems. It represents the amount of recoverable energy after storage; it is the ratio of energy leaving to energy entering the system, shown in equation (12).

$$\eta_{round-trip} = \frac{E_{out}}{E_{in}} = \frac{P_{out} t_{out}}{P_{in} t_{in}} \quad (12)$$

While literature has generally considered the round-trip efficiency of adiabatic-type CAES to be approximately 70% [13,31], the analysis presented in [32] provides a realistic efficiency approximation of around 60%.

In addition to round-trip efficiency, the system's exergy can be analyzed to gauge energy quality and identify the location and magnitude of losses in the system. It is a useful tool for thermal system designers, as an exergy analysis provides greater detail for how individual components in a system perform; an analysis only focusing on round-trip efficiency does not provide the same information. Once evaluated, designers can use the results to pinpoint and address particular components to improve systems. Exergy analyses consider the surroundings of the system, measuring energy potential with respect to the environment. On a unit mass basis, thermo-mechanical exergy is calculated by equation (13).

$$x = (u - u_0) + p_0(v - v_0) - T_0(s - s_0) + \frac{\bar{V}^2}{2} + gz \quad (13)$$

In real processes, exergy is not conserved; it can be destroyed due to irreversibilities. As exergy destruction represents the total magnitude of losses, its minimization would result in more effective use of energy in a system. In general, exergy destruction is calculated using equation (14). Exergy in the system was evaluated for each component to illustrate its loss contribution. A thorough description of exergy, its analysis and destruction can be found in [33].

$$X_D = X_{in} - X_{out} \quad (14)$$

#### 4.0 RESULTS AND DISCUSSION

Using the developed system model, the round trip efficiency and the total exergy destroyed for the baseline case was evaluated to be 56.2% and 9.2 GJ, respectively. Parameter variations were applied to the system model; the resulting round trip efficiency and total exergy destruction changes are shown in Figure 5 for four design parameters. The four parameters showed noticeable deviation from baseline when subject to varying design values. An increase in round-trip efficiency and a decrease in total exergy destruction are considered beneficial to improving the system.

In Figure 5(a), the variation of the measured values – the round-trip efficiency and total exergy destruction – with respect to different system depths is shown. As air is stored deeper, the system performance increases. However, as the depth increases, the round-trip efficiency and total exergy destruction begins to reach a constant value of approximately 1.01 and 0.97, respectively, relative to the baseline value. This result can be attributed largely to the decrease in required stored air mass, given in Figure 6.

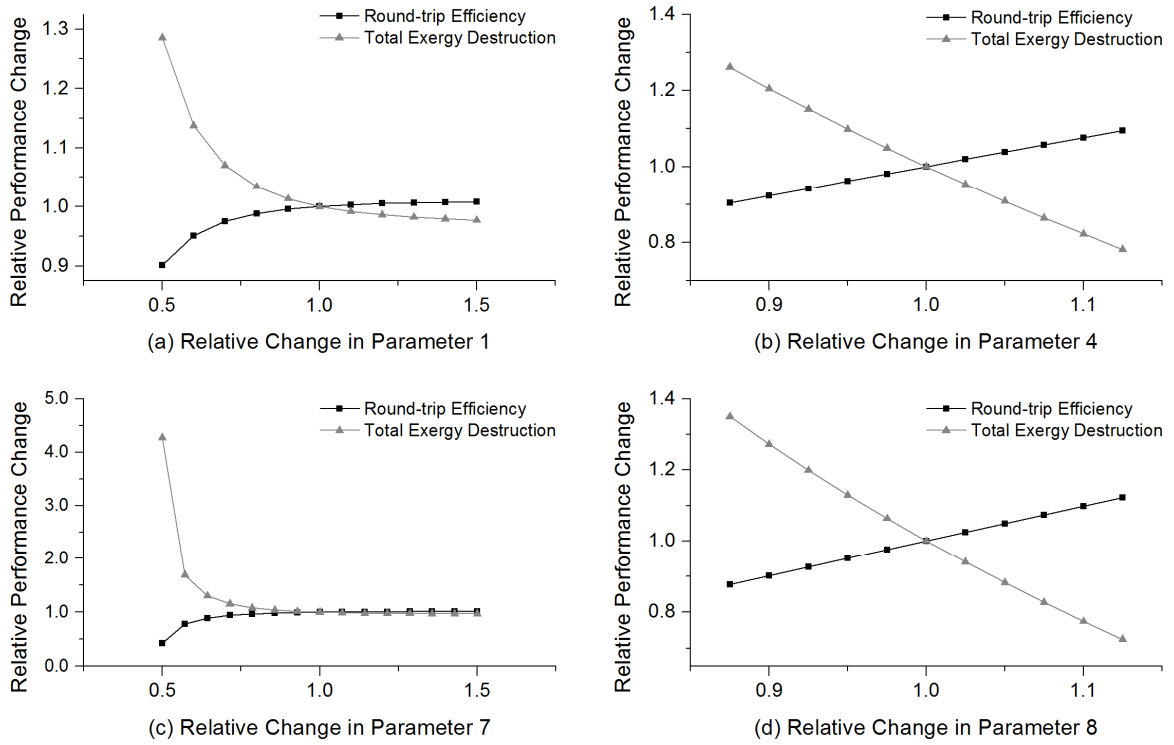


**Figure 5** – Relative change in round-trip efficiency and total exergy destruction due to parameter variation

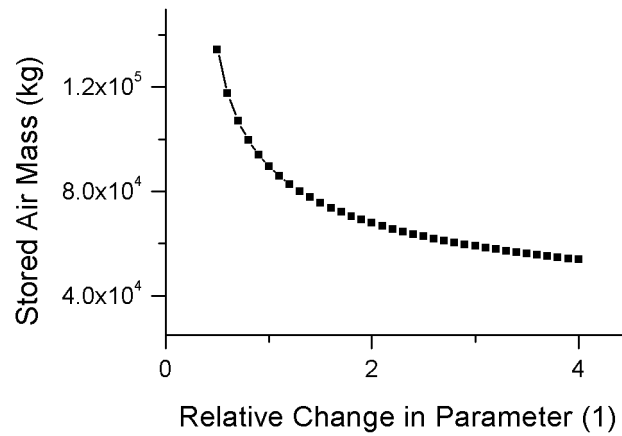


**Figure 6** – Mass vs. depth

Figures 5(b) and 5(d) illustrate the effect of varying compressor and expander isentropic efficiencies on system performance. In Figure 5(c), the system performance improves as the pipe size increases. The asymptotical relationship given in the figure is



typical of pipe flows as the increase in pipe diameter reduces flow velocities resulting in decreasing frictional losses.

Expanding on the information for the design parameters given in Figure 5, Figure 7 displays the contribution to total exergy destruction of each system component modelled at each design point. This provides a direct comparison of the losses experienced in each of the components as design parameters vary.

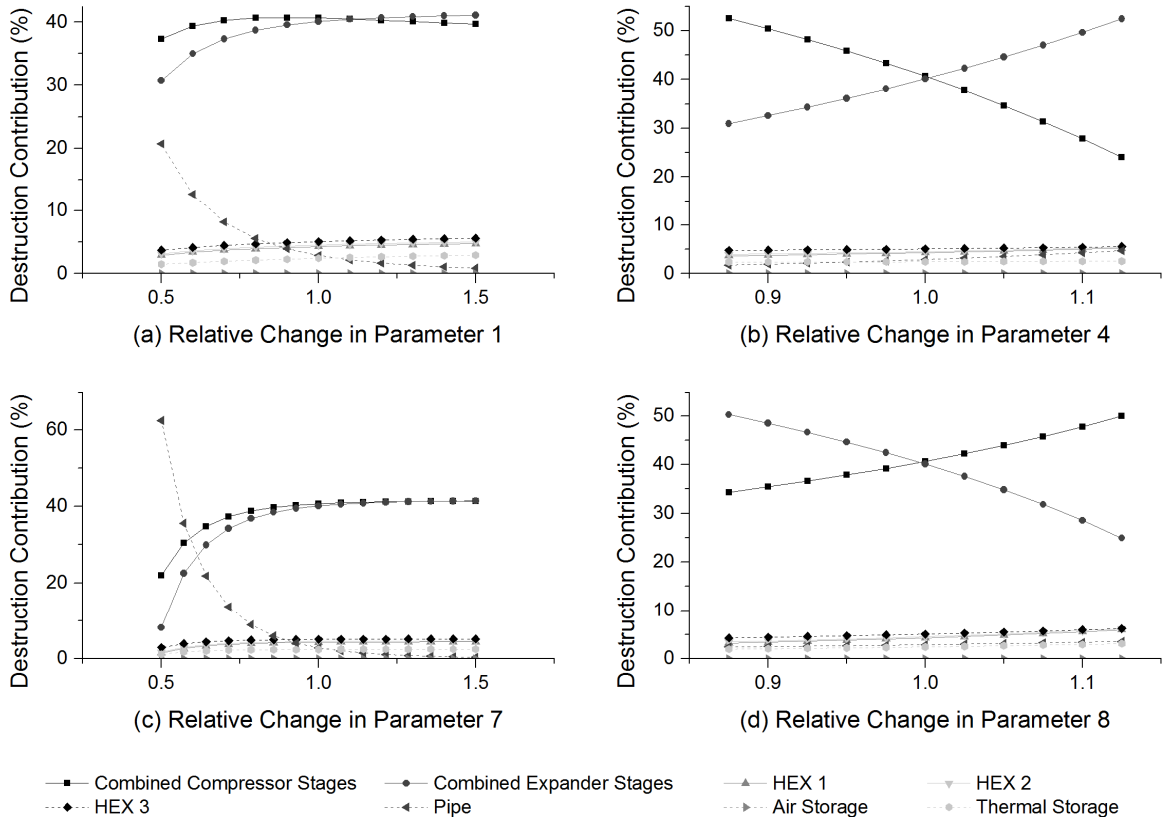


**Figure 7** – Component contribution to total exergy destruction

In Figures 7(a), 7(b) and 7(d), the air compression and expansion stages were the dominant contributors to exergy destruction in the system. As the air storage depth increases in Figure 7(a), the exergy destruction contribution from the compressor and turbine both peak at approximately 40%. The air compressor exergy destruction contribution then begins to decrease starting at 0.8 relative to the baseline storage depth.

This trend occurs due to a reduction in total exergy destroyed in the compression stages combined with an increase in total exergy destruction during heat exchange. Figures 7(b) and 7(d) demonstrate similar results, with the contributions coming from the air compressor and turbine swapped. Figure 7(c) shows the exergy destruction contribution from pipe sizing significantly decreasing as diameters are increased.

A comparison of the results of all analyzed parameters is found in Figure 8. This figure plots the maximum extent that round-trip efficiency and total exergy destruction deviates from the simulated system's baseline value over the parametric variation range prescribed in Table 2.

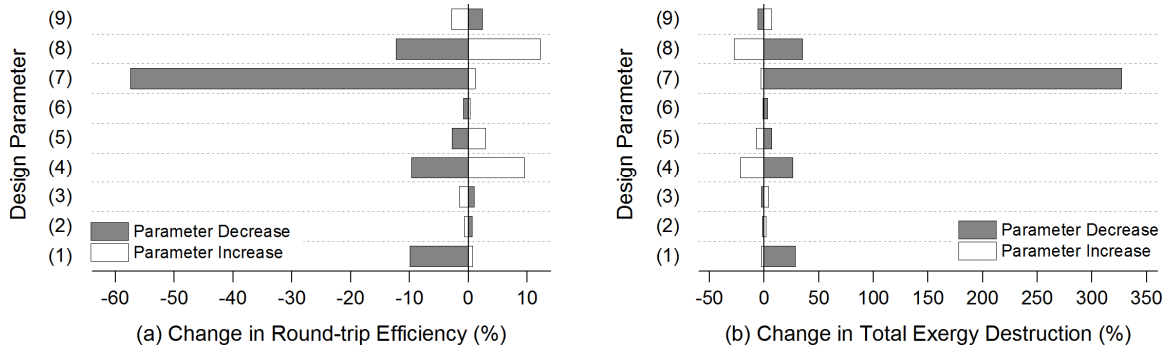


**Figure 8** – Extent of deviation in (a) round-trip efficiency and (b) total exergy destruction from baseline

Among all the analyzed parameters, an increase expander and compressor isentropic efficiencies, and maximum HEX extraction temperature ratio yielded higher round-trip efficiencies and lower exergy destruction. Conversely, a decrease in pipe size, expander and compressor isentropic efficiencies, air storage depth, and maximum HEX extraction temperature ratio resulted in a lower round-trip efficiency and greater exergy destruction. The decrease in system performance is particularly drastic in the case of smaller pipe diameters.

Figure 9 shows the sensitivity of round-trip efficiency and total exergy destruction to the design parameters. The sensitivity of each parameter is represented by its sensitivity index – a number between 0 and 1 with higher values being showing greater significance [34].

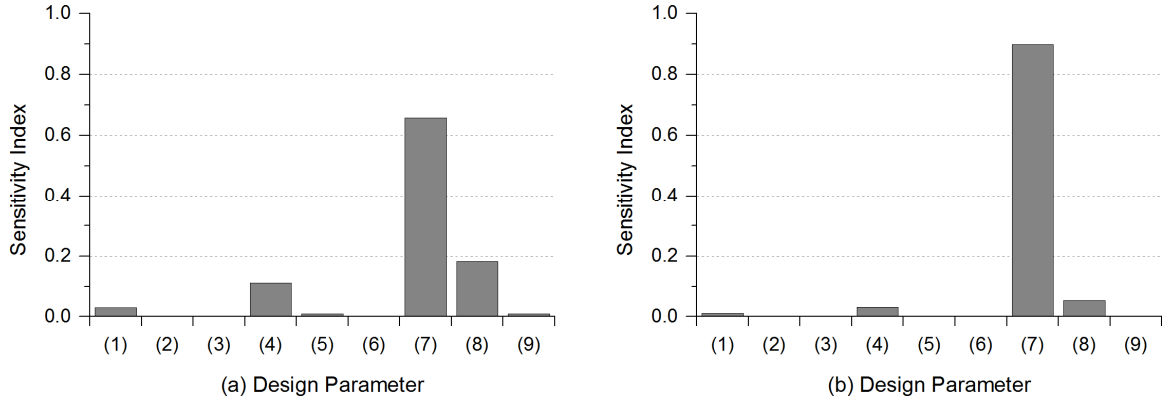


**Figure 9** – Sensitivity of (a) round-trip efficiency, (b) total exergy destruction to design parameters

Figure 9 confirms what is shown in Figure 8, that the system is most sensitive to pipe diameter over the design parameter range of variation. Expander and compressor isentropic efficiencies and depths are the other parameters that play significant roles in the system. The sensitivity analysis found that maximum HEX extraction temperature ratio was not significant relative to the other parameters.

Figure 10 expands on the data given in Figure 9(b), showing a breakdown of the exergy destruction sensitivity of each component to the design parameters in the simulated UWCAES system. It highlights the number of components that are susceptible to a clear performance fluctuation through parametric variation of the design.

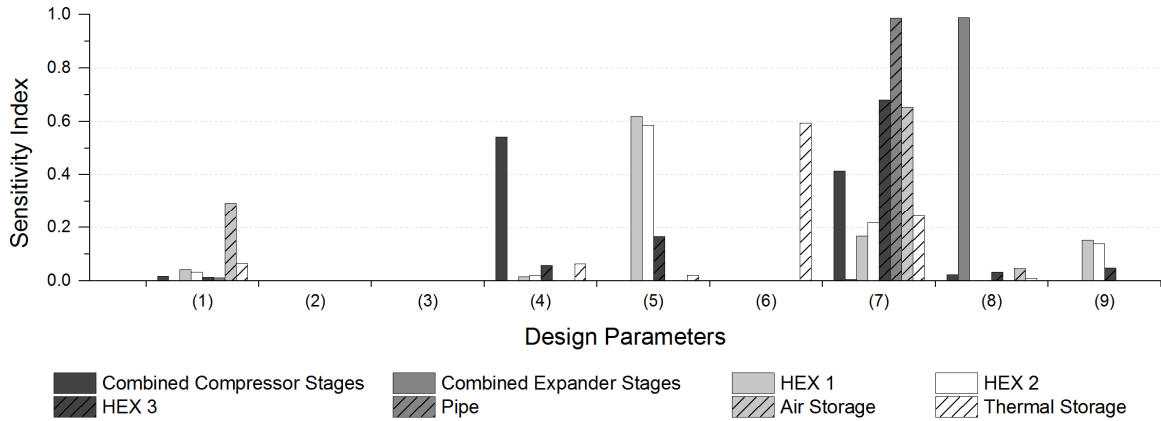


**Figure 10** – Sensitivity of system component exergy destruction to design parameters

From the figure, most of the UWCAES system components were sensitive to pipe diameter changes, with some components having a sensitivity index greater than or equal to approximately 0.4. In comparison, only a few components showed sensitivity to the variation in each of the other design parameters.

Based on the findings shown in the previous figures, it can be said that pipe sizing has the greatest potential to impact UWCAES system performance, followed by the turbine and compressor efficiency and depth. Changes in the other parameters showed small, incremental performance gains that may not be beneficial; a detailed capital and operational cost analysis may demonstrate this point.

This analysis demonstrates that careful consideration of pipe design is required. The model system examined pressure losses using a single header pipe setup. However, it is expected that more complex pipe networks will be used in operating UWCAES systems, especially at larger scales. The effect of pressure loss in a UWCAES is system-wide; greater losses would require the air compressor to consume more energy and discharge air at higher pressures as compensation, in addition to a reduction in energy output during system discharge. As such, UWCAES designs should have efforts made to minimize pressure losses.

For noticeable performance gains, turbines and compressors with better isentropic efficiencies should be used; this would reduce their energy requirements. Utilizing heat exchangers that capture more thermal energy would also increase system performance, albeit to a lesser extent. When improvements in these parameters are combined, the system performance greatly benefits. To illustrate this, when the three parameters are set to their upper value of the analysis range, the system achieves a round-trip efficiency of approximately 71% and experiences roughly a 50% reduction in total exergy destruction relative to the base case.

It is possible to conclude that the given baseline value for the air storage depth and pipe diameter may be optimal with respect to the other parameters, as further increases in these parameters do not have any significant effect on system performance. In addition, due to the sharp performance degradation associated with shallower water depths and smaller pipe sizes, it would be ideal for any UWCAES system being designed to only use these parameters' optimum values.

## **5.0 CONCLUSIONS**

UWCAES is a novel adaptation of mature CAES technology showing promise for energy storage. Its isobaric and scalable characteristics can assist CAES application at smaller scales and to wider audiences. A basic system was modelled and an analysis of primary system design parameters has been presented. Results of the model were studied to determine the magnitude of impact and parameter sensitivity. It was found that the pipe diameter, turbine, air compressor and air storage depth exerted the greatest influence on system performance. Despite pipe diameter being most sensitive, increases in pipe size from the base case yielded marginal gains. For the simulated model, significant gains in performance can be achieved through the engagement of more efficient turbo-expanders and air compressors. Some performance gains can also be

realized through more effective heat recovery. As well, it is worth noting that the accumulator depth plays a notable role in determining system performance until a critical depth is reached, beyond which round trip efficiency begins to stabilize.

The analysis conducted in the paper offers some utility for elementary UWCAES system design. The parametric study and sensitivity analysis provide insight into where resources should be directed in the interest of optimizing round trip efficiency.

## **ACKNOWLEDGEMENTS**

Research and development of the UWCAES system is being conducted in partnership with Hydrostor Inc. Funding for this study was provided by the Ontario Centres of Excellence. We appreciate their guidance and support throughout the project.

## **REFERENCES**

- [1] K. Porter, C. Mudd, and M. Weisburger, “Review of international experience integrating variable renewable energy generation,” Apr. 2007.
- [2] A. J. Cavallo, “Energy Storage Technologies for Utility Scale Intermittent Renewable Energy Systems,” *Journal of Solar Energy Engineering*, vol. 123, no. 4, pp. 387–389, Jul. 2001.
- [3] M. Beaudin, H. Zareipour, A. Schellenberglobe, and W. Rosehart, “Energy storage for mitigating the variability of renewable electricity sources: An updated review,” *Energy for Sustainable Development*, vol. 14, no. 4, pp. 302–314, Dec. 2010.
- [4] K. Hedegaard and P. Meibom, “Wind power impacts and electricity storage – A time scale perspective,” *Renewable Energy*, vol. 37, no. 1, pp. 318–324, Jan. 2012.
- [5] F. Díaz-González, A. Sumper, O. Gomis-Bellmunt, and R. Villafafila-Robles, “A review of energy storage technologies for wind power applications,” *Renewable and Sustainable Energy Reviews*, vol. 16, no. 4, pp. 2154–2171, May 2012.
- [6] A. Evans, V. Strezov, and T. J. Evans, “Assessment of utility energy storage options for increased renewable energy penetration,” *Renewable and Sustainable Energy Reviews*, vol. 16, no. 6, pp. 4141–4147, Aug. 2012.

- [7] Electricity Advisory Committee, “Bottling Electricity: Storage as a Strategic Tool for Managing Variability and Capacity Concerns in the Modern Grid,” 2008.
- [8] S. Koohi-Kamali, V. V Tyagi, N. A. Rahim, N. L. Panwar, and H. Mokhlis, “Emergence of energy storage technologies as the solution for reliable operation of smart power systems: A review,” *Renewable and Sustainable Energy Reviews*, vol. 25, pp. 135–165, Jun. 2013.
- [9] R. Baxter, *Energy Storage - A Nontechnical Guide*. PennWell, 2007.
- [10] S. van der Linden, “Bulk energy storage potential in the USA, current developments and future prospects,” *Energy*, vol. 31, no. 15, pp. 3446–3457, Dec. 2006.
- [11] S. Sundararagavan and E. Baker, “Evaluating energy storage technologies for wind power integration,” *Solar Energy*, vol. 86, no. 9, pp. 2707–2717, Sep. 2012.
- [12] H. Chen, T. N. Cong, W. Yang, C. Tan, Y. Li, and Y. Ding, “Progress in electrical energy storage system: A critical review,” *Progress in Natural Science*, vol. 19, no. 3, pp. 291–312, Mar. 2009.
- [13] S. Succar and R. Williams, “Compressed Air Energy Storage: Theory, Resources and Applications for Wind Power,” Apr. 2008.
- [14] F. Crotogino, K.-U. Mohmeyer, and R. Scharf, “Huntorf CAES: more than 20 years of successful operation,” 2001.
- [15] L. Davis and R. Schainker, “Compressed Air Energy Storage (CAES): Alabama Electric Cooperative McIntosh Plant - Overview and Operational History,” 2006.
- [16] C. Jakiel, S. Zunft, and A. Nowi, “Adiabatic compressed air energy storage plants for efficient peak load power supply from wind energy: the European project AA-CAES,” *International Journal of Energy Technology and Policy*, vol. 5, no. 3, pp. 296–306, 2007.
- [17] B. Cheung, R. Cariveau, and D. S.-K. Ting, “Storing energy underwater,” *Mechanical Engineering*, vol. 134, no. 12, pp. 38–41, Dec-2012.
- [18] Y. M. Kim, D. G. Shin, and D. Favrat, “Operating characteristics of constant-pressure compressed air energy storage (CAES) system combined with pumped hydro storage based on energy and exergy analysis,” *Energy*, vol. 36, no. 10, pp. 6220–6233, Nov. 2011.
- [19] T. F. Havel, “Adsorption-enhanced compressed air energy storage,” in *Nanotech 2011*, 2011, vol. 1, pp. 759–762.

- [20] Y. M. Kim and D. Favrat, “Energy and exergy analysis of a micro-compressed air energy storage and air cycle heating and cooling system,” *Energy*, vol. 35, no. 1, pp. 213–220, Jan. 2010.
- [21] H. Ibrahim, R. Younès, A. Ilinca, M. Dimitrova, and J. Perron, “Study and design of a hybrid wind–diesel-compressed air energy storage system for remote areas,” *Applied Energy*, vol. 87, no. 5, pp. 1749–1762, May 2010.
- [22] J. J. Proczka, K. Muralidharan, D. Villela, J. H. Simmons, and G. Frantziskonis, “Guidelines for the pressure and efficient sizing of pressure vessels for compressed air energy storage,” *Energy Conversion and Management*, vol. 65, pp. 597–605, Jan. 2013.
- [23] L. Zhang, S. Ahmari, M. Budhu, and B. Sternberg, “Feasibility Study of Compressed Air Energy Storage Using Steel Pipe Piles,” in *GeoCongress 2012*, 2012, pp. 4272–4279.
- [24] R. J. Seymour, “Ocean Energy On-Demand Using Underocean Compressed Air Storage,” in *ASME 2007 26th International Conference on Offshore Mechanics and Arctic Engineering*, 2007, vol. 5, pp. 527–531.
- [25] A. Pimm and S. Garvey, “Analysis of flexible fabric structures for large-scale subsea compressed air energy storage,” *Journal of Physics: Conference Series*, vol. 181, no. 1, p. 012049, Aug. 2009.
- [26] A. J. Pimm, S. D. Garvey, and R. J. Drew, “Shape and cost analysis of pressurized fabric structures for subsea compressed air energy storage,” *Proceedings of the Institution of Mechanical Engineers, Part C: Journal of Mechanical Engineering Science*, vol. 225, no. 5, pp. 1027–1043, May 2011.
- [27] B. Cheung, N. Cao, R. Cariveau, and D. S.-K. Ting, “Distensible air accumulators as a means of adiabatic underwater compressed air energy storage,” *International Journal of Environmental Studies*, vol. 69, no. 4, pp. 566–577, Aug. 2012.
- [28] H. Ibrahim, A. Ilinca, and J. Perron, “Energy storage systems—Characteristics and comparisons,” *Renewable and Sustainable Energy Reviews*, vol. 12, no. 5, pp. 1221–1250, Jun. 2008.
- [29] R. K. Shah and D. P. Sekulic, *Fundamentals of Heat Exchanger Design*. John Wiley & Sons, Inc., 2003, p. 976.
- [30] Y. A. Çengel and J. M. Cimbala, *Fluid Mechanics: Fundamentals and Applications*. McGraw-Hill Higher Education, 2006, p. 956.



- [31] G. Grazzini and A. Milazzo, “Thermodynamic analysis of CAES/TES systems for renewable energy plants,” *Renewable Energy*, vol. 33, no. 9, pp. 1998–2006, Sep. 2008.
- [32] N. Hartmann, O. Vöhringer, C. Kruck, and L. Eltrop, “Simulation and analysis of different adiabatic Compressed Air Energy Storage plant configurations,” *Applied Energy*, vol. 93, pp. 541–548, May 2012.
- [33] A. Bejan and M. J. Moran, *Thermal Design and Optimization*. New York: Wiley, 1996.
- [34] A. Saltelli, M. Ratto, T. Andres, F. Campolongo, J. Cariboni, D. Gatelli, M. Saisana, and S. Tarantola, *Global Sensitivity Analysis. The Primer*. 2008.

## CHAPTER IV

# MULTI-OBJECTIVE OPTIMIZATION OF AN UNDERWATER COMPRESSED AIR ENERGY STORAGE SYSTEM USING A GENETIC ALGORITHM

BRIAN C. CHEUNG, RUPP CARRIVEAU<sup>1</sup>, DAVID S-K. TING

Turbulence and Energy Laboratory, Ed Lumley Centre for Engineering Innovation,  
University of Windsor, Ontario, Canada, N9B 3P4

Under review for publication in the journal “Energy”

## NOMENCLATURE

|              |  |               |  |
|--------------|--|---------------|--|
| $A$          | Heat transfer surface area, m <sup>2</sup>   | $p$           | Pressure, kPa  |
| $C$          | Thermal capacitance, kJ/K                    | $q$           | Heat transfer rate, kW                                 |
| $\dot{C}$    | Cost rate, \$/h                              | $R$           | Gas constant, kJ/kg•K                                  |
| $c$          | Average cost per unit exergy, \$/MWh         | $\dot{S}$     | Entropy rate, kJ/K                                     |
| $c_p$        | Constant pressure specific heat, kJ/kg•K     | $s$           | Specific entropy, kJ/kg•K                              |
| $c_v$        | Constant volume specific heat, kJ/kg•K       | $T$           | Temperature, K   |
| $CRF$        | Capital recovery factor                      | $TR$          | Charge-to-discharge time ratio                         |
| $\dot{Ex}$   | Exergy rate, kW                              | $t$           | Time, h  |
| $ex$         | Specific exergy, kJ/kg                       | $U$           | Overall heat transfer coefficient, W/m <sup>2</sup> •K |
| $g$          | Gravitational acceleration, m/s <sup>2</sup> | $V$           | Volume, m <sup>3</sup>                                 |
| $H$          | Annual operating hours, h                    | $v$           | Specific volume, m <sup>3</sup> /kg                    |
| $h$          | Specific enthalpy, kJ/kg                     | $\dot{W}$     | Work, kW   |
| $IR$         | Interest rate, %                             | $w$           | Specific work, kJ/kg                                   |
| $k$          | Specific heat ratio                          | $w_i$         | Pseudo-weight  |
| $\dot{m}$    | Mass flow rate, kg/s                         | $Z$           | Equipment cost, \$                                     |
| $m_{air}$    | Stored air mass, kg                          | $\dot{Z}$     | Capital cost rate, \$/h                                |
| $MCF$        | Maintenance cost factor                      | $z$           | Depth below water surface, m                           |
| $N$          | System life, years                           |               |  |
| $N_{stages}$ | Number of compressor/expander stages         | <b>Greek</b>  |  |
| $n$          | Polytropic exponent                          | $\beta_i$     | Stage pressure ratio                                   |
| $NTU$        | Number of transfer units                     | $\varepsilon$ | Heat exchanger effectiveness (%)                       |
| $OP$         | Operating profit, \$/cycle                   | $\eta$        | Efficiency (%)   |
| $P$          | Power, kW                                    |               |  |

<sup>1</sup> Corresponding author. Tel: +1 519 253 3000. Email address: rupp@uwindsor.ca

**Subscripts**

|     |             |     |               |
|-----|-------------|-----|---------------|
| $0$ | Reference   | $F$ | Fuel          |
| $c$ | Compressor  | $Q$ | Heat transfer |
| $D$ | Destruction | $P$ | Product       |
| $e$ | Expander    | $W$ | Work          |

**1.0 INTRODUCTION**

Growing interest in electrical energy storage (EES) technologies highlights a changing paradigm in the management of electricity resources. As the electricity grid system experiences renewal and modernization, grid owners and operators are looking to implement large-scale energy storage technologies. As well, governments have begun the process of mandating electricity storage into energy planning policies [1,2]. The benefits of EES are significant; since storage decouples electricity production and demand, EES systems provide many valuable grid support services which include shifting peak demands, regulating electricity flow, reducing transmission and distribution congestion, and integrating renewable energy generation [3–5].

An emerging technology in the field of EES is underwater compressed air energy storage (UWCAES). It is a novel application of conventional compressed air energy storage (CAES) where a series of air compressors and turbo-expanders are used to convert electrical energy to and from compressed air. The novelty of the UWCAES concept lies in the method of storing the compressed air; air is stored in a series of submerged distensible air accumulators placed near the beds of deep water bodies rather than in rigid reservoirs, such as underground geologic formations. Building on the advantages of conventional CAES – low energy costs due to its inexpensive storage media and large storage capacity [6,7] – the UWCAES concept offers two important design characteristics: a scalable design and isobaric system charge and discharge profiles [8]. A few researchers have investigated the application of submerged, distensible air accumulators for UWCAES. Pimm and Garvey [9] determined an

optimum shape of a large-scale axisymmetric fabric structure by minimizing the ratio between the energy bag cost and stored energy. In their modelling, the stresses on the bag membrane were analyzed, and costs of the required material were calculated. Pimm et al. [10] later extended their analysis using finite-element analysis modelling. Cheung et al. [8] performed a field-study of the distensible air accumulator.

Sustainability is an important concern in energy systems, particularly energy storage. As both energy demand and costs increase, solutions that attempt to address these two issues must be efficient and cost-effective. Therefore, it is critical that any solution designed must be optimized for these conditions. The aim of this paper is to present a multi-objective optimization of a theoretical UWCAES system using a genetic algorithm that determines an optimal system configuration based on three objectives:

1. Maximizing overall round-trip efficiency of the system
2. Minimizing the cost rate of the system
3. Maximizing the operating profit of the system as it participates in energy arbitrage

Using the principles of thermodynamics and economics, the UWCAES system was numerically simulated by major components and optimized for a series of design variables. Energy, exergy, and exergoeconomic analyses were performed to provide a foundation for evaluating the objectives. Furthermore, a sensitivity analysis of the economic effect of interest rate on optimal system configurations was studied. The goal of the numerical model presented in this study was to simulate the high-level performance of the overall system during an operation cycle; the findings of this paper can serve as a foundation for future low-level UWCAES plant design optimizations analyzed by highly refined models.

Optimization using multi-objective genetic algorithms (MOGA) is particularly useful in the design of real-world engineering systems, which typically have several, at often times conflicting, goals and objectives. While optimizations can be done individually for each objective, solutions may be dominated by certain objectives over others and the cost of time and resources required may prove prohibitively expensive. Instead, MOGAs can be employed to find solutions that balance the trade-offs of each objective in a timely and cost-effective manner by a stochastic search process that mimics biological evolution – particularly Darwin’s rule of natural selection [11].

The application of genetic algorithms in optimizing thermal system designs has been a relatively recent development dating back to mid-1990. In one of the earliest instances, Schmit et al. [12] applied a genetic algorithm (GA) to the design of an avionic compact high intensity cooler. The optimization objective was to balance fluid pressure drop and overall thermal resistance based on the geometric design of the cooler. The proliferation of thermoeconomic/exergoeconomic optimization that started during the same time period has led optimization studies applying genetic algorithms [13,14].

Toffolo and Lazzaretto [15] were among the first to introduce the methodology for performing multi-objective thermoeconomic optimization using evolutionary algorithms. In their study, the CGAM problem [16] was simultaneously optimized for exergetic efficiency and total cost rate. Their study was later extended to incorporate an environmental objective [17]. Researchers have went on to apply the multi-objective approach to other types of thermal energy systems, such as combined cycle power systems [18–21], and components, like heat pumps [22,23] and heat recovery steam generators [24].

The application of genetic algorithm-type optimization technique to energy storage systems has been very limited to date. Among the few studies, Borghi et al. [25]

optimized a high-temperature superconducting magnetic energy storage device based on the amount of conductor and the device volume. An evolution strategy minimization algorithm was applied for two different optimization methods. Morandin et al. [26] applied a MOGA optimization to the design of a thermo-electric energy storage system, where investment costs were minimized and round-trip efficiency maximized.

## **2.0 SIMULATING & ANALYZING UWCAES**

UWCAES is the latest development in energy storage technology. Using the principles established by conventional CAES systems operating in Huntorf, Germany [27] and McIntosh, Alabama, USA [28], in combination with aspects from the developing adiabatic CAES concept, UWCAES is poised to bring CAES applications to smaller scales while eliminating fossil fuel use. A general system consists of five main components – an air compressor, turbine, motor/generator, thermal recovery unit (TRU) and storage – that facilitate the compression and expansion of air. The UWCAES system process is given in Figure 1.

The system operates in three distinct phases: charge, storage, and discharge. When the system is being charged to store energy, ambient air is drawn into the system, compressed, and stored in the submerged air accumulators. The TRU, consisting of heat exchangers and thermal storage, extracts and stores thermal energy generated during the compression process. While in storage, air pressure is maintained by the hydrostatic forces exerted on the air mass by the surrounding water [8]. When energy is needed, air is first discharged from storage, heated up by the TRU, and expanded through a generator-connected turbine, producing an electrical output.

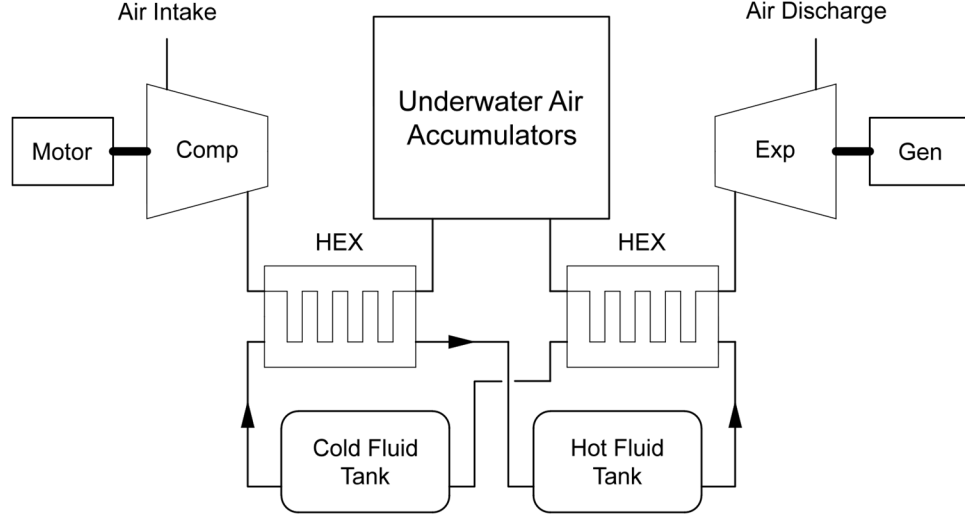


**Figure 1** - The general UWCAES process

## 2.1 Thermal Performance

The air storage pressure,  $p_{storage}$ , is a dictating factor of UWCAES systems. Air stored in the submerged accumulators is bounded hydrostatically to the pressure exerted by water at depth  $z$ , given in equation (1).

$$p_{storage} = p_{atm} + \rho_{water}gz \quad (1)$$

The system's energy capacity is dependent on the stored air mass,  $m_{air}$ . The air mass can be calculated using the ideal gas law, given that flow of air in the system is an isobaric process and remains at low temperatures and pressures. It is assumed that air in storage reaches thermal equilibrium with the water temperature,  $T_{water}$ , at depth.

$$m_{air} = \frac{(pV)_{storage}}{RT_{water}} \quad (2)$$

Multistage configurations are typically used to achieve large pressure ratios during air compression and expansion. The pressure ratio for each stage,  $\beta_i$ , can be

expressed by equation (3), assuming that all  $N$  stages in an air compressor or turbine are identical.

$$\beta_i = \left( p_{discharge} / p_{inlet} \right)^{1/N} \quad (3)$$

The process in which air is compressed or expanded is considered to be polytropic, given in equation (4). The polytropic exponent,  $n$ , can be calculated using equation (5) if the isentropic efficiency,  $\eta_{isentropic}$ , is known.

$$pv^n = const. \quad (4)$$

$$n = \left[ 1 - \frac{1}{\log \beta_i} \log \left( 1 + \frac{1}{\eta_{isentropic}} \left( \beta_i^{(k-1)/k} - 1 \right) \right) \right]^{-1} \quad (5)$$

where the specific heat ratio  $k = c_p / c_v$  and has a typical value for air of 1.4.

The performance of air compression and expansion in multistage configurations can be estimated using equations (6) and (7). The performance is quantified by air discharge temperature,  $T_2$ , and specific work,  $w$ .

$$T_2 = T_1 \beta_i^{(n-1)/n} \quad (6)$$

$$w = \int_1^2 v \, dp = \frac{nR(T_2 - T_1)}{n-1} = \frac{nRT_1}{n-1} \left( \beta_i^{(n-1)/n} - 1 \right) \quad (7)$$

Having obtained the air mass required and specific work of the compression or expansion stage, the operational charge and discharge times,  $t_{charge}$  and  $t_{discharge}$ , respectively, can be determined using equation (8) as a function of power requirements.

$$t = \frac{m_{air} w}{P} \quad (8)$$



As it is with adiabatic CAES systems, thermal recovery is used to eliminate the need for fuel combustion when preheating air for expansion [29]. Heat exchangers used in thermal recovery must be adequately sized to regulate temperatures during the compression and expansion processes; this helps to protect and enhance performance of the pneumatic equipment. Methods prescribed in design resources [30, 31] can be used to size or evaluate heat exchanger performance. For the model in this study, the effectiveness-NTU method was used to size the flat plate heat exchangers during air compression and rate their performance during air expansion. The effectiveness-NTU method can be evaluated using equations (9) and (10), which express the heat exchanger effectiveness  $\mathcal{E}$  and number of transfer units  $NTU$ , respectively.

$$\mathcal{E} = \frac{q}{q_{\max}} \quad (9)$$

$$NTU = \frac{UA}{C_{\min}} \quad (10)$$

## 2.2 Exergy Analysis

Exergy analysis is a useful tool to gauge energy quality and identify the location and magnitude of losses in a system process. It provides greater detail on how components in a system perform – information that eludes energy analyses. In a thermo-mechanical system, exergy of substances can be divided into three components – physical, kinetic and potential [32]. For this study, the latter two forms of exergy were considered negligible.

An exergy rate balance, shown in equation (11), can be obtained by applying the first and second laws of thermodynamics for all sources of exergy, expressed as an exergy rate  $\dot{X}$ , acting in a control volume during a process.

$$\sum_i \dot{Ex}_i - \sum_e \dot{Ex}_e + \dot{Ex}_W + \dot{Ex}_Q - \dot{Ex}_D = \Delta \dot{Ex} \quad (11)$$

where the subscripts W, Q, and D denote exergy rates associated with work, heat transfer, and destruction, respectively. The terms of equation (11) are defined using equations (12) through (16).

$$\dot{Ex} = \dot{m}x \quad (12)$$

$$ex = ex_{PH} = (h - h_0) - T_0(s - s_0) \quad (13)$$

$$\dot{Ex}_W = \dot{W} \quad (14)$$

$$\dot{Ex}_Q = \left(1 - \frac{T_0}{T}\right) \dot{Q} \quad (15)$$

$$\dot{Ex}_D = T_0 \dot{S}_{gen} \quad (16)$$

Equations (14) and (15) illustrates how exergy quantifies the usefulness or value of an energy source. As work energy can be converted into other forms of energy like heat, it is more useful, thus its exergy value is greater. Conversely, since heat energy is limited in its uses, it has a lower exergy value. Unlike energy, exergy is not conserved. Its destruction, as given in equation (16), is a useful quantity when analyzing a system, as it accounts for irreversibilities in a thermodynamic process. System designs can be improved when exergy destruction is minimized.

### 2.3 Exergoeconomic Analysis

Exergoeconomics combines exergy analysis and economic principles on a component level to provide information crucial to the design and operation of a cost-effective system. While thermodynamic analysis methods can determine losses through quantifying exergy destruction, it is more practical to associate a cost to the

inefficiencies. Each flow is defined by a cost rate  $\dot{C}$ , given in equation (17). The cost rate is the product of the exergy rate and the cost per unit exergy,  $c$ .

$$\dot{C} = c\dot{X} \quad (17)$$

Once all flow cost rates have been found, a cost balance is written for each component, defined by equation (18).

$$\sum_e \dot{C}_e + \dot{C}_w = \dot{C}_Q + \sum_i \dot{C}_i + \dot{Z} \quad (18)$$

In exergoeconomic analysis, two unique streams are defined – the fuel and product stream. The product refers to the stream produced from a system, while fuel is the stream consumed to generate the product. These terms are used when defining the cost of exergy destruction. In equation (18), there is no cost term directly associated with exergy destruction; it is a hidden cost. When the exergy and exergoeconomic cost rate balances are combined, the expression for cost of exergy destruction can be expressed as either a function of the fuel or product, shown in equation (19) and (20), respectively.

$$\dot{C}_D = c_F \dot{E}x_D \quad (19)$$

$$\dot{C}_D = c_P \dot{E}x_D \quad (20)$$

The choice of which exergy destruction cost rate equation is used depends on how fuel and product streams are interpreted. Equation (19) is used if the product stream is fixed; additional fuel would be required to produce the product when accounting for exergy destruction. Equation (20) assumes that the fuel stream is fixed; exergy destruction is considered as a loss of product. In practice, these equations approximate the average costs associated with exergy destruction with equation (19) yielding a lower estimate and equation (20) yielding a higher estimate in most applications [32]. The actual exergy destruction cost is somewhere between the two.

The cost of equipment,  $Z$ , is comprised of two components – purchased and operating and maintenance (O&M) costs. It is incorporated into the exergoeconomic analysis as a cost rate  $\dot{Z}$ , determined using the annualized (levelized) cost method [33], represented by the capital recovery factor  $CRF$ . The method distributes the equipment costs over the annual operational time across the system's service life. This is expressed using equations (21) and (22).

$$\dot{Z} = \frac{Z(MCF)(CRF)}{H} \quad (21)$$

$$CRF = \frac{IR(1+IR)^N}{(1+IR)^N - 1} \quad (22)$$

### 3.0 MULTI-OBJECTIVE GENETIC ALGORITHM OPTIMIZATION

Optimization routines seek to find optimal system solutions based on its design parameters. In the application of genetic algorithms, the design parameters are referred to as decision variables. Boundaries can be placed on the decision variable values to aid the search for optimum solutions. A design vector, referred to as an individual, is created from the decision variables and their respective boundaries. The generation of the individual is stochastic, as values of the decision variables are randomly assigned.

Compared to other optimization methods, genetic algorithms are well suited for practical optimization problems, since real world problems typically have a discrete value restriction on the decision variables. As well, genetic algorithms can efficiently solve many types of optimization problems, handle discontinuous objective functions, and do not rely on initial solution guesses [34]. Genetic algorithms achieve these characteristics by evaluating objective (fitness) functions with a group of individuals, known as a population. Researchers have developed genetic algorithm variants over the

past few decades that mainly differ in how new individuals and populations are generated [35]. However, the basic working process of each variant remains the same, given in Figure 2. For this study, the multi-objective optimization was performed using a controlled elitist genetic algorithm [36]. It is a variant of NSGA-II, which is one of the more frequently used MOGAs [37].

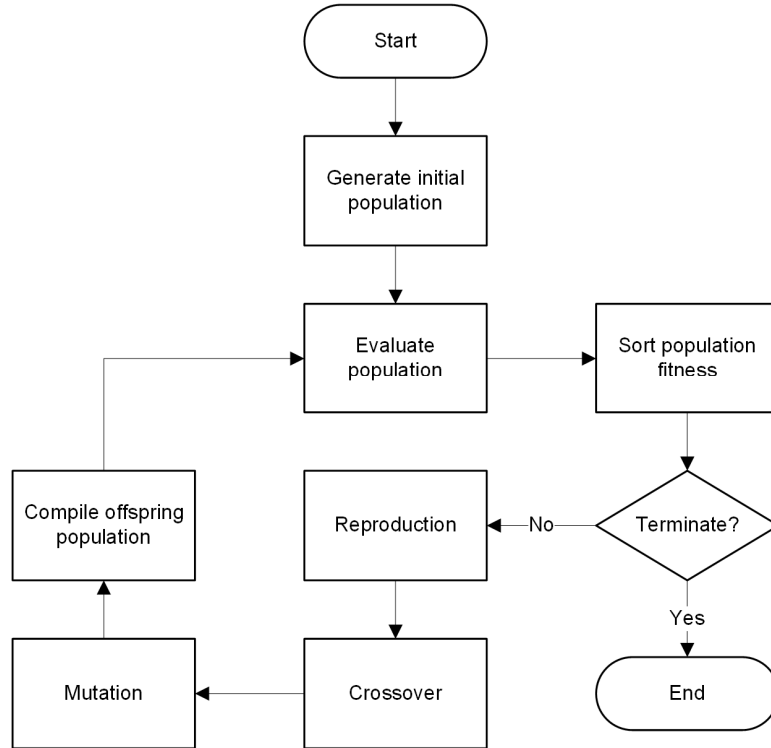


**Figure 2** - The basic process flow of a genetic algorithm

### 3.1 Optimization Process

The optimization begins with the generation of an initial population. The genetic algorithm will evaluate the population with respect to the objective functions to compute each individual's fitness value. A sorting process based on the theory of natural selection is used. A pair of solutions are picked and compared against each other for the following two conditions:

1. The first solution is no worse than the second solution in all objectives.

2. The first solution is strictly better than the second solution in at least one objective.

If both conditions hold true, it can be said that the first solution dominates the second solution. The sorting process evaluates all solutions to determine those that are not dominated.

Termination conditions are checked to determine if further iterations are required. These conditions can include limits on fitness, time, generations, and function tolerance. While no termination condition is satisfied, the genetic algorithm proceeds to generate an offspring population from the current population set. Otherwise, the optimization returns the non-dominated solutions, which are called Pareto-optimal solutions. A set of Pareto-optimal solutions is referred to as the Pareto-optimal front. An example of these two concepts is given in Figure 3.

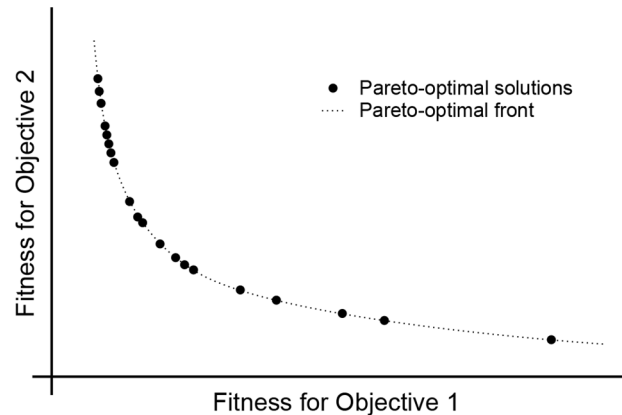


**Figure 3** - A Pareto-optimal front

The offspring population with new individuals is generated using the genetic operations of reproduction, crossover and mutation. In reproduction, the best solutions are copied over to the new population, whereas crossover generates a single offspring solution from a pair of parents in the current population. For mutation, offspring

solutions are created by replacing the value of a decision variable in an individual with the hope that the new individual is improved.

Many different variants of multi-objective genetic algorithms exist; for this study, the elitist non-dominated sorting genetic algorithm, known as NSGA-II, was used. In NSGA-II, a crowded tournament selection operator enhances the genetic operations. It determines two metrics – a non-domination rank and local crowding distance – for each individual in the current population. The crowding distance is a measure of the empty search space around an individual. Two random individuals will compete in a tournament, with the winner being the one that has a better rank or same rank and greater crowding distance; this process is intended to mimic natural selection. Additional details on the NSGA-II procedure can be found in [34] and [38].

### **3.2 Multiple Criterion Decision Making**

Once the optimization is completed and a Pareto-optimal solution set is obtained, post-processing is performed to determine a single preferred solution. The pseudo-weight vector approach described in [34] is one of a variety of post-optimal decision making methods used to determine an applicable solution when higher-level considerations (e.g. societal, political, etc.) are factored in. It is worth noting that there are a number of techniques available that can find a preferred solution while an optimization procedure is running.

A pseudo-weight vector is calculated for each solution and is compared to user-defined weights for all objectives. The preferred solution is one whose pseudo-weights are the closest to that of the user-defined weights. The pseudo-weights are based on the solution's fitness values relative to the entire solution set. Equation (23) is used to calculate a solution's weight  $w_i$  of the  $i^{\text{th}}$  objective function.

$$w_i = \frac{(f_i^{\max} - f_i(x)) / (f_i^{\max} - f_i^{\min})}{\sum_{m=1}^M (f_m^{\max} - f_m(x)) / (f_m^{\max} - f_m^{\min})} \quad (23)$$

where M is the total number of objectives.

#### 4.0 CASE STUDY

A 4 MWh UWCAES system with air accumulators situated 5 km offshore and 100 m below the water surface in a fresh water lake was simulated and optimized using MATLAB R2012b and the Global Optimization Toolbox. The basic layout of the system is given in Figure 4, where mechanical equipment handling the energy conversion is situated on-shore is attached to a header pipe. The header pipe is assumed to run along the lake bedding and is attached to each accumulator using feeder pipes.

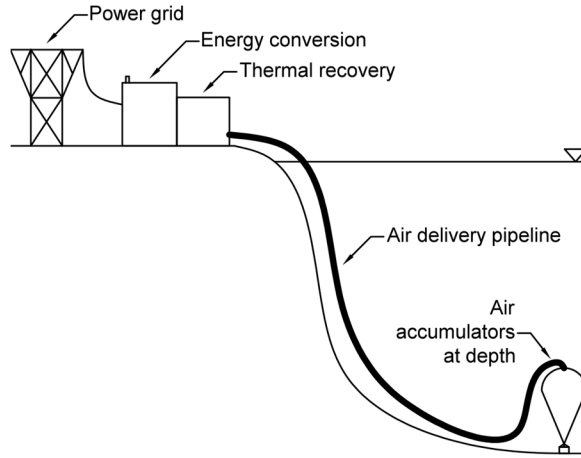


**Figure 4** - A UWCAES system with on-shore equipment

#### 4.1 Modelling Approach

Each component of the UWCAES process was evaluated in the numerical model; the compression phase heat exchangers, thermal storage tank, and air accumulator



capacity were sized, whereas the performance of the air compressors, air expanders, expansion phase heat exchangers and header pipe were rated.

The quantity of heat exchangers used in the system equalled to the number of compression stages and were designed for 95% effectiveness during system charge. The heat exchangers were of a flat-plate design operating in laminar counter-flow to minimize pressure loss and maximize fluid extraction temperature. The heat exchanger units served as intercoolers during air compression and pre-heaters during air expansion and were applied in reverse order during preheating. Thermal energy was stored in a 60% ethylene glycol solution.

Air was stored in a series of accumulators. The number of accumulators used was based on the required storage capacity and the accumulator unit volume. Heated ethylene glycol was stored in an insulated vertical cylinder storage tank with a diameter of 6 m and was evaluated for heat loss during storage. The capacity of the tank was sized based on the amount of stored fluid.

## 4.2 System Variables

The numerical model evaluated system designs based the decision variables as specified in Table 1. Additional variables required for analyzing a system design are given in Table 2; these variables remain constant throughout the optimization process.

**Table 1** - Decision Variables

| Variable                                | Lower Boundary | Upper Boundary |
|---|----------------|----------------|
| System power input, $P_{in}$ (kW)       | 1000           | 3000           |
| Number of air compression stages, $N_c$ | 1              | 6              |
| Header pipe diameter, $D_{pipe}$ (mm)   | 300            | 600            |
| Number of air expansion stages, $N_e$   | 1              | 6              |
| Charge-to-discharge time ratio*, TR     | 1              | 2              |

\* TR =  $t_{charge}/t_{discharge}$

**Table 2** - Additional analysis variables

| <b>Variable</b>   | <b>Value</b> |
|---|--------------|
| Reference temperature, $T_o$ (°C)                               | 8            |
| Reference pressure, $p_o$ (kPa)                                 | 101.325      |
| Water temperature at depth, $T_{\text{water}}$ (°C)             | 8            |
| Air accumulator unit volume, $V_{\text{acc}}$ (m <sup>3</sup> ) | 50           |
| System storage time, $t_{\text{storage}}$ (hours)               | 8            |
| Header pipe roughness, $e$ (mm)                                 | 0.003        |
| Compressor isentropic efficiency, $\eta_c$ (%)                  | 87.5         |
| Compressor motor efficiency, $\eta_{\text{motor}}$ (%)          | 95           |
| Expander isentropic efficiency, $\eta_e$ (%)                    | 87.5         |
| Expander generator efficiency, $\eta_{\text{gen}}$ (%)          | 97           |
| System lifespan, $N$ (years)                                    | 15           |
| Interest rate, $IR$ (%)   | 10           |
| Maintenance cost factor, $MCF$                                  | 1.06         |

Economic conditions, particularly interest rates, can affect the design of a system. To gauge the economic impact interest rates have on the optimization results and preferred system designs, a sensitivity analysis was performed for annual interest rates ranging from 5 to 15%.

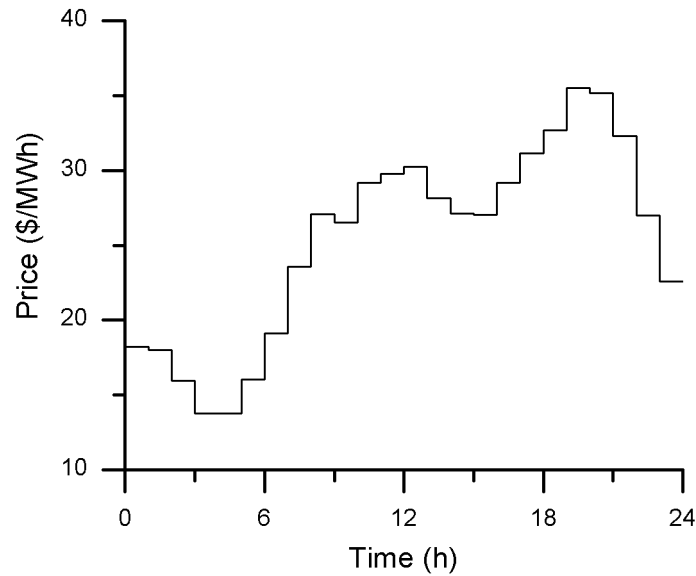
### 4.3 Cost Functions

The system model was evaluated for energy, exergy, and exergoeconomics. The equipment cost functions used in the exergoeconomic evaluation are provided in Table 3. Quotes from various equipment manufacturers and cost index data sourced from the US Bureau of Labor Statistics were used to develop and modify cost functions found in previous literature. In general, the cost functions used show that costs increase as equipment scales or inputs increase. For the air compressor and expander cost functions, its costs are also dependant on the isentropic efficiency.

**Table 3** - Equipment cost functions [26,32]

| Component                 | Function   |
|---------------------------|--|
| Air accumulator           | $Z_{acc} = 6500 N_{acc}$   |
| Air compressor            | $Z_{comp} = \left( \frac{232.63 \dot{m}_c}{0.90 - \eta_c} \right) \left( \frac{p_{out}}{p_{in}} \right) \ln \left( \frac{p_{out}}{p_{in}} \right)$ |
| Air expander              | $Z_{exp} = \left( \frac{1054.42 \dot{m}_e}{0.92 - \eta_e} \right) \ln \left( \frac{p_{in}}{p_{out}} \right) [1 + \exp(0.036 T_{in} - 54.4)]$       |
| Flat plate heat exchanger | $Z_{HEX} = 146000 \left( \frac{A_{HEX}}{2946} \right)^{0.6}$   |
| Pipe                      | $Z_{pipe} = 3.6 L_{pipe} \exp(0.00864 D_{pipe})$   |
| Thermal storage tank      | $Z_{tank} = 4500 V_{tank}^{0.6} + 10000$   |

An hourly average electricity price profile over 24 hours, given in Figure 5, was developed using data for the year of October 2012/October 2013 in Ontario, Canada. The data was sourced from Ontario's Independent Electricity System Operator. The modelled system calculated an average electricity price based on charge and discharge times, which corresponded to off-peak and peak prices, respectively.

**Figure 5** - Average hourly electricity prices over 24-hours

#### 4.4 Optimization Objectives

UWCAES system designs were optimized for three objectives and are given in Table 4.

**Table 4** – Summary of objective functions

| Parameter                   | Function   | Goal     |
|-----------------------------|--|----------|
| Round-trip efficiency (%)   | $\eta_{roundtrip} = (E_{out}/E_{in}) \times 100\%$             | Maximize |
| Total cost rate (\$/h)      | $\dot{C}_{total} = \sum (\dot{C}_D + \dot{Z})$                 | Minimize |
| Operating profit (\$/cycle) | $OP = c_{peak,avg} t_{discharge} - c_{offpeak,avg} t_{charge}$ | Maximize |

The first objective was to maximize system round-trip efficiency, which analyzed the amount of energy provided by the system to the amount used to store energy. It is an important parameter when comparing energy storage systems. The round-trip efficiency is based on the energy balance of the UWCAES system.

The second objective was the minimization of a cumulative cost rate function consisting of exergy destruction and capital costs rates associated with every component in the system. A design with a lower total cost rate would imply better operational efficiency and lower capital costs.

The last objective was maximizing operating profit that a system design would receive following an operation cycle. A cycle is the cumulative operational times for system charge, storage and discharge. The function determined favourable operation schedules based on electricity prices.

#### 4.5 Modelling and Optimization Considerations

Several assumptions were made in the numerical system sizing and simulation.

- All processes were steady-state and had steady flows.
- Pressure losses associated with feeder pipes and pipe fittings were negligible.

- Ethylene glycol did not experience any thermal stratification during storage.
- Costs were evaluated as present value.
- Equipment did not have a salvage value at the end of the operating lifespan.

## 5.0 RESULTS

The Pareto-optimal solution set obtained from the multi-objective optimization model using the objectives outlined in section 4.4 is given in Figure 6. It can be seen that the Pareto-optimal solution set can form a three-dimensional surface. Figures 7 and 8 provide some two-dimensional views of the three-dimensional scatter plot. It can be seen that the Pareto-optimal system designs had round-trip efficiencies ranging from 57.8% to 70.7%, total costs rates between \$60.57 to \$887.69 per hour, and operating profits from \$14.01 to \$63.54 per cycle.

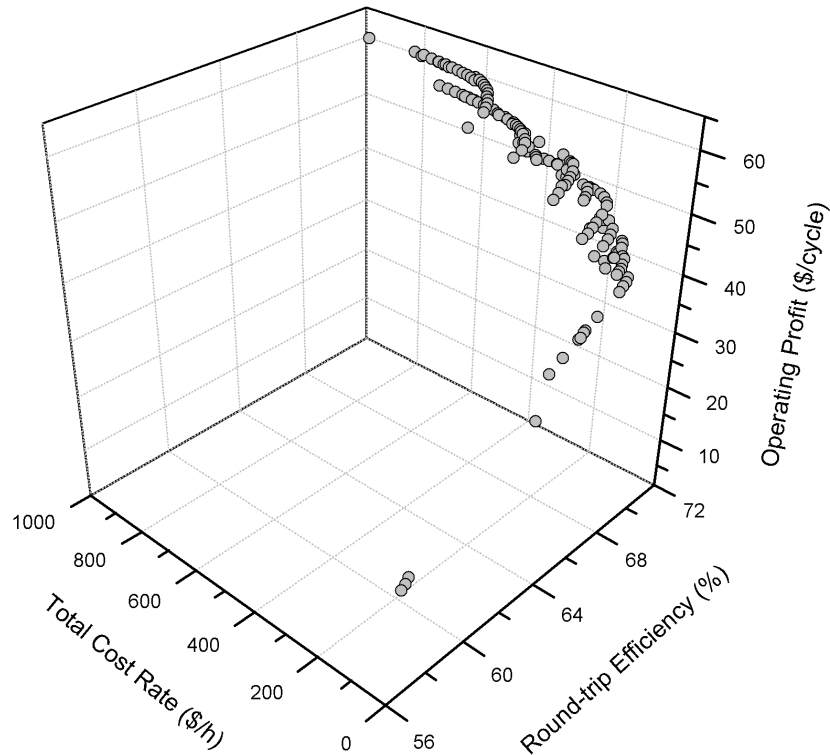


**Figure 6** - Pareto-optimal solutions (IR = 10%)

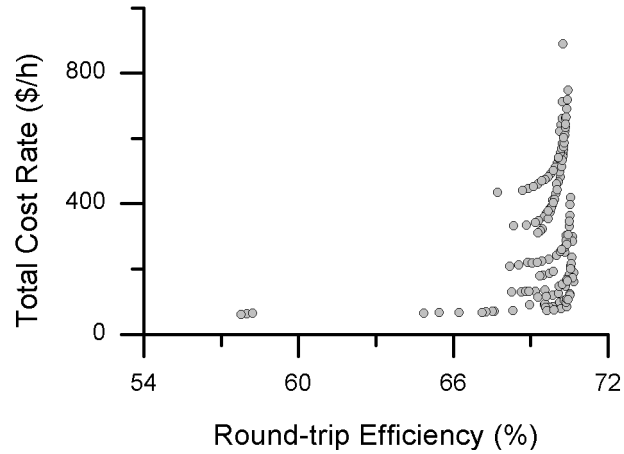


**Figure 7** - Total Cost Rate vs. Round-trip Efficiency

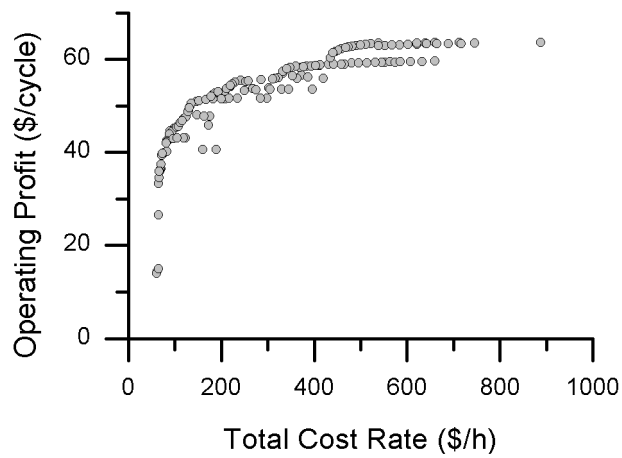


**Figure 8** - Operating Profit vs. Total Cost Rate

In Figure 7, the observed Pareto front shows the correlation between round-trip efficiency and total cost rate. The total cost rate of the system increases marginally as the round-trip efficiency approaches approximately 67%. For round-trip efficiencies over 67%, the total cost rate increases significantly. The Pareto front shows an approximate asymptotic value for maximum round-trip efficiency and minimum cost rate at 70.7% and \$60.5/h, respectively.

Figure 8 provides a comparison between the operating profit and total cost rate of a system. In general, the graph follows a logarithmic trend with a maximum operating profit of approximately \$63.6/cycle. The asymptotic values shown by the previous two figures demonstrate the maximum performance the modelled system can achieve.

An interest rate sensitivity analysis on the Pareto-optimal solution set, given in Figure 9, shows the total cost rate rising with interest rates. This can be attributed to the higher capital costs for the components. Based on the optimization results, the Pareto-optimal front along the total cost rate increases by a factor of approximately 1.3 for every 5% increase in interest rate. The effect of interest rate on the round-trip efficiency and operating profit appears negligible.

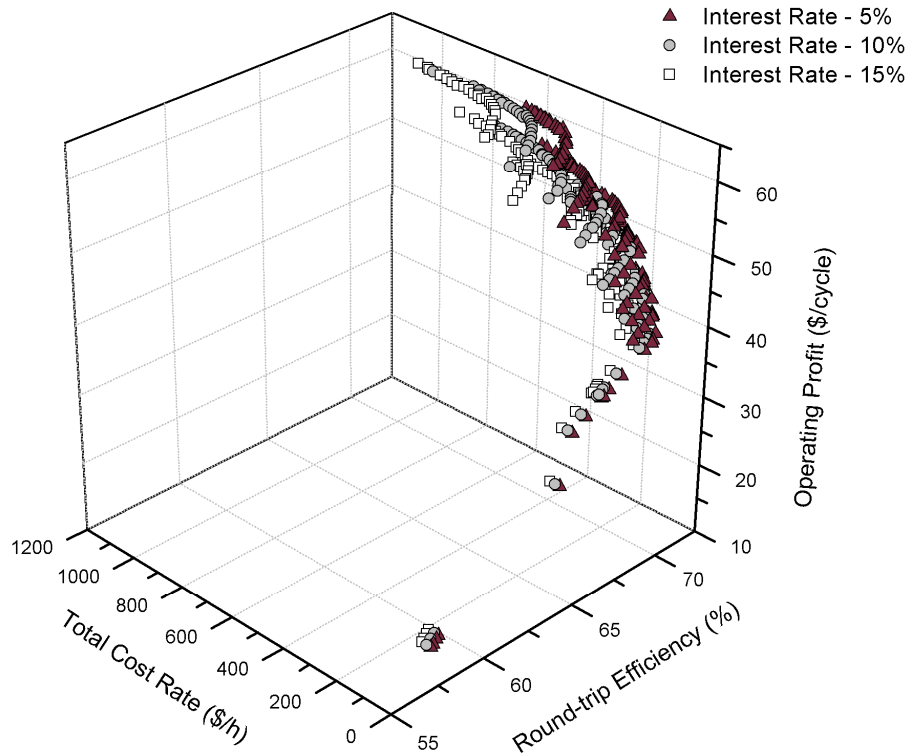


**Figure 9** - Pareto-optimal solutions (IR = 5% to 15%)

The results chosen by the decision making method are summarized in Table 5. Preferred designs were chosen for each interest rate that was analyzed using the pseudo-weight vector approach. The designs were determined with the assumption that all three optimization objectives modelled were equally important/weighted.

**Table 5** – Selected system design summary at different interest rates

| $IR$ (%) | $P_{in}$ (kW) | $N_c$ | $D_{pipe}$ (mm) | $N_e$ | $TR$ |
|----------|---------------|-------|-----------------|-------|------|
| 5        | 1968          | 3     | 360             | 4     | 1.0  |
| 10       | 1967          | 3     | 320             | 3     | 1.0  |
| 15       | 1967          | 3     | 340             | 3     | 1.0  |

**Table 6** - Performance of the selected system designs at different interest rates

| $IR$ (%) | $\eta_{roundtrip}$ (%) | $\dot{C}_{total}$ (\$/h) | $OP$ (\$/cycle) |
|----------|------------------------|--------------------------|-----------------|
| 5        | 68.88                  | 162.57                   | 54.06           |
| 10       | 68.20                  | 208.91                   | 53.17           |
| 15       | 68.81                  | 277.83                   | 53.67           |

Common attributes in the design of a preferred system at the modelled interest rates can be observed. The preferred systems shows similar designed power input, number of air compression stages, and identical charge-discharge time ratios. Slight differences are seen in the header pipe diameter and number of air expansion stages. At 5% interest rate, the preferred system used a bigger pipe diameter and an additional expansion stage when compared to the base case ( $IR = 10\%$ ). This configuration resulted in a marginally higher round-trip efficiency and operating profit, and a 22.2% decrease in total cost rate. It can be concluded that at lower interest rates, better components can be used. At 15% interest rate, the preferred system designed featured a bigger pipe size, corresponding to a 33.0% increase in the total cost rate from the base case. Accordingly, the round-trip efficiency and cycle operating profit increased slightly.



## **6.0 CONCLUSIONS**

Evaluating and optimizing the energy, exergy, and exergoeconomics of a UWCAES system has provided some valuable insight into its design. The energy analysis provides high-level details for system performance. The exergy analysis identifies the sources of energy loss. Exergoeconomics associates an economic value to the losses. When used in an optimization model, a balance between performance, energy losses, and costs can be made effectively.

The results of the multi-objective optimization of a UWCAES with the objectives of maximizing round-trip efficiency and operating profit, and minimizing cost rate has yielded a set of optimum designs. These designs have slight variations for different interest rates. When averaging the preferred designs for the different interest rates, this study found a general optimum system design to use a power input of 1967 kW, three air compression stages, a 340 mm header pipe, three expansion stages, and a charge-discharge time ratio of 1.0. These results are not absolute; the findings of the optimization model should serve as recommendations for a designer to determine an appropriate system design in a timely manner.

## **ACKNOWLEDGEMENTS**

The authors would like to acknowledge support provided by Hydrostor Inc. and Ontario Centres of Excellence. Along with funding, research and development of the UWCAES system is being conducted in partnership with Hydrostor Inc.

## **REFERENCES**

- [1] California Public Utilities Commission, "CPUC Sets energy storage goals for utilities," 2013. [Online]. Available:

<http://docs.cpuc.ca.gov/PublishedDocs/Published/G000/M079/K171/79171502.PDF>.

- [2] D. Frankel, "South Korea considers mandatory energy storage and electricity rate restructuring," *SmartGridNews*, 2013. [Online]. Available: [http://www.smartgridnews.com/artman/publish/Business\\_Policy\\_Regulation/South-Korea-considers-mandatory-energy-storage-and-electricity-rate-restructuring-6088.html/#.UmAKMZf92vB](http://www.smartgridnews.com/artman/publish/Business_Policy_Regulation/South-Korea-considers-mandatory-energy-storage-and-electricity-rate-restructuring-6088.html/#.UmAKMZf92vB). [Accessed: 17-Oct-2013].
- [3] J. Eyer and G. Corey, "Energy Storage for the Electricity Grid: Benefits and Market Potential Assessment Guide," Sandia National Laboratories, 2010.
- [4] Electricity Advisory Committee, "Bottling Electricity: Storage as a Strategic Tool for Managing Variability and Capacity Concerns in the Modern Grid," US Department of Energy, 2008.
- [5] S. Koohi-Kamali, V. V Tyagi, N. A. Rahim, N. L. Panwar, and H. Mokhlis, "Emergence of energy storage technologies as the solution for reliable operation of smart power systems: A review," *Renew. Sustain. Energy Rev.*, vol. 25, pp. 135–165, Jun. 2013.
- [6] S. Sundararagavan and E. Baker, "Evaluating energy storage technologies for wind power integration," *Sol. Energy*, vol. 86, no. 9, pp. 2707–2717, Sep. 2012.
- [7] H. Chen, T. N. Cong, W. Yang, C. Tan, Y. Li, and Y. Ding, "Progress in electrical energy storage system: A critical review," *Prog. Nat. Sci.*, vol. 19, no. 3, pp. 291–312, Mar. 2009.
- [8] B. Cheung, N. Cao, R. Cariveau, and D. S.-K. Ting, "Distensible air accumulators as a means of adiabatic underwater compressed air energy storage," *Int. J. Environ. Stud.*, vol. 69, no. 4, pp. 566–577, Aug. 2012.
- [9] A. Pimm and S. Garvey, "Analysis of flexible fabric structures for large-scale subsea compressed air energy storage," *J. Phys. Conf. Ser.*, vol. 181, no. 1, p. 012049, Aug. 2009.
- [10] A. J. Pimm, S. D. Garvey, and R. J. Drew, "Shape and cost analysis of pressurized fabric structures for subsea compressed air energy storage," *Proc. Inst. Mech. Eng. Part C J. Mech. Eng. Sci.*, vol. 225, no. 5, pp. 1027–1043, May 2011.
- [11] A. Abraham, L. Jain, and R. Goldberg, *Evolutionary Multiobjective Optimization*. Springer London, 2005, p. 302.

- [12] T. S. Schmit, A. K. Dhingra, F. Landis, and G. Kojasoy, "Genetic algorithm optimization technique for compact high intensity cooler design," *J. Enhanc. Heat Transf.*, vol. 3, no. 4, pp. 281–290, 1996.
- [13] M. Valdés, M. D. Durán, and A. Rovira, "Thermoeconomic optimization of combined cycle gas turbine power plants using genetic algorithms," *Appl. Therm. Eng.*, vol. 23, no. 17, pp. 2169–2182, Dec. 2003.
- [14] H. Li, R. Nalim, and P.-A. Haldi, "Thermal-economic optimization of a distributed multi-generation energy system—A case study of Beijing," *Appl. Therm. Eng.*, vol. 26, no. 7, pp. 709–719, 2006.
- [15] A. Toffolo and A. Lazzaretto, "Evolutionary algorithms for multi-objective energetic and economic optimization in thermal system design," *Energy*, vol. 27, no. 6, pp. 549–567, Jun. 2002.
- [16] A. Valero, M. A. Lozano, L. Serra, G. Tsatsaronis, J. Pisa, C. Frangopoulos, and M. R. von Spakovsky, "CGAM problem: Definition and conventional solution," *Energy*, vol. 19, no. 3, pp. 279–286, 1994.
- [17] A. Lazzaretto and A. Toffolo, "Energy, economy and environment as objectives in multi-criterion optimization of thermal systems design," *Energy*, vol. 29, no. 8, pp. 1139–1157, 2004.
- [18] P. Roosen, S. Uhlenbruck, and K. Lucas, "Pareto optimization of a combined cycle power system as a decision support tool for trading off investment vs. operating costs," *Int. J. Therm. Sci.*, vol. 42, no. 6, pp. 553–560, Jun. 2003.
- [19] P. Ahmadi, I. Dincer, and M. A. Rosen, "Exergy, exergoeconomic and environmental analyses and evolutionary algorithm based multi-objective optimization of combined cycle power plants," *Energy*, vol. 36, no. 10, pp. 5886–5898, 2011.
- [20] P. Ahmadi, A. Almasi, M. Shahriyari, and I. Dincer, "Multi-objective optimization of a combined heat and power (CHP) system for heating purpose in a paper mill using evolutionary algorithm," *Int. J. Energy Res.*, vol. 36, no. 1, pp. 46–63, Jan. 2012.
- [21] A. G. Kaviri, M. N. M. Jaafar, and T. M. Lazim, "Modeling and multi-objective exergy based optimization of a combined cycle power plant using a genetic algorithm," *Energy Convers. Manag.*, vol. 58, pp. 94–103, Jun. 2012.
- [22] H. Sayyaadi, E. H. Amlashi, and M. Amidpour, "Multi-objective optimization of a vertical ground source heat pump using evolutionary algorithm," *Energy Convers. Manag.*, vol. 50, no. 8, pp. 2035–2046, Aug. 2009.

- [23] R. Murr, H. Thieriot, A. Zoughaib, and D. Clodic, "Multi-objective optimization of a multi water-to-water heat pump system using evolutionary algorithm," *Appl. Energy*, vol. 88, no. 11, pp. 3580–3591, 2011.
- [24] R. Carapellucci and L. Giordano, "A comparison between exergetic and economic criteria for optimizing the heat recovery steam generators of gas-steam power plants," *Energy*, vol. 58, pp. 458–472, Sep. 2013.
- [25] C. A. Borghi, M. Fabbri, and P. L. Ribani, "Design optimization of a microsuperconducting magnetic energy storage system," *IEEE Trans. Magn.*, vol. 35, no. 5, pp. 4275–4284, 1999.
- [26] M. Morandin, M. Mercangöz, J. Hemrle, F. Maréchal, and D. Favrat, "Thermoeconomic design optimization of a thermo-electric energy storage system based on transcritical CO<sub>2</sub> cycles," *Energy*, vol. 58, pp. 571–587, Sep. 2013.
- [27] F. Crotogino, K.-U. Mohmeyer, and R. Scharf, "Huntorf CAES: more than 20 years of successful operation," in *Solution Mining Research Institute Meeting, Orlando, FL, 23–25 April, 2001*.
- [28] L. Davis and R. Schainker, "Compressed Air Energy Storage (CAES): Alabama Electric Cooperative McIntosh Plant - Overview and Operational History," in *Electricity Storage Association Meeting: Energy Storage in Action, Knoxville, TN, 2006*.
- [29] C. Jakiel, S. Zunft, and A. Nowi, "Adiabatic compressed air energy storage plants for efficient peak load power supply from wind energy: the European project AA-CAES," *Int. J. Energy Technol. Policy*, vol. 5, no. 3, pp. 296–306, 2007.
- [30] A. Bejan and A. D. Kraus, *Heat Transfer Handbook*. John Wiley & Sons, Inc., 2003, p. 1496.
- [31] R. K. Shah and D. P. Sekulic, *Fundamentals of Heat Exchanger Design*. John Wiley & Sons, Inc., 2003, p. 976.
- [32] A. Bejan and M. J. Moran, *Thermal Design and Optimization*. New York: Wiley, 1996.
- [33] Y. A. Gogus, "Thermoeconomic optimization," *Int. J. Energy Res.*, vol. 29, no. 7, pp. 559–580, Jun. 2005.
- [34] K. Deb, *Multi-Objective Optimization Using Evolutionary Algorithms*. John Wiley & Sons, Inc., 2001, p. 518.

- [35] S. Elsayed, R. Sarker, and D. Essam, "A Comparative Study of Different Variants of Genetic Algorithms for Constrained Optimization," in *Simulated Evolution and Learning SE - 18*, vol. 6457, K. Deb, A. Bhattacharya, N. Chakraborti, P. Chakraborty, S. Das, J. Dutta, S. Gupta, A. Jain, V. Aggarwal, J. Branke, S. Louis, and K. Tan, Eds. Springer Berlin Heidelberg, 2010, pp. 177–186.
- [36] The MathWorks Inc., *Global Optimization Toolbox User's Guide*, R2012b ed. 2012.
- [37] H. Ishibuchi and Y. Nojima, "Comparison between Single-Objective and Multi-Objective Genetic Algorithms: Performance Comparison and Performance Measures," in *2006 IEEE International Conference on Evolutionary Computation*, 2006, pp. 1143–1150.
- [38] K. Deb, A. Pratap, S. Agarwal, and T. Meyarivan, "A fast and elitist multiobjective genetic algorithm: NSGA-II," *IEEE Trans. Evol. Comput.*, vol. 6, no. 2, pp. 182–197, Apr. 2002.

## CHAPTER V

# CONCLUSIONS AND RECOMMENDATIONS

### 1.0 SUMMARY AND CONCLUSIONS

It is crucial for energy systems to be well designed in terms of performance, efficiency, and costs. As such, studies on the design and optimization of an UWCAES system have been presented.

In Chapter 2, the working principles and advantages of the UWCAES concept over conventional CAES was discussed, and the application of a submerged, distensible air accumulator was examined. The pilot project conducted showed the performance of the balloon-shaped air accumulator when subjected to field conditions. It was determined that the charge and discharge behaviour of the accumulators were predictable with some variation in flow rates and pressures during the cycling of air. A slight air pressure drop during discharge was observed; this was most likely attributed to the vertical hydrostatic pressure difference between the top and bottom of the accumulator. It can be concluded that this behaviour can be mitigated by an improved accumulator design.

Chapter 3 presented a sensitivity analysis of design parameters on a theoretical UWCAES system. A basic system was modelled and analyzed for energy and exergy. Performance was quantified by the system's overall round-trip efficiency and exergy destruction. Results of the parametric study revealed that the pipe diameter, air turbine/expander, air compressor and air storage depth exerted the greatest influence on system performance. While pipe diameter was the most sensitive, any increases in the parameter from the baseline yielded marginal gains. Instead, addressing the efficiency of the turbo-expanders and air compressors could attain significant performance gains. It is

worth mentioning that critical values were achieved in some design parameters, namely air storage depth.

Optimal system configurations were determined in Chapter 4 using a multi-objective optimization model employing a genetic algorithm. A numerical simulation of varying UWCAES system configurations was performed in MATLAB, with each configuration evaluated for energy, exergy, and exergoeconomics. Optimization objectives were formulated from the thermodynamic analyses that focused on maximizing round-trip efficiency and operating profit, and minimizing a total cost rate based on equipment capital costs and exergy destruction. For a 4 MWh UWCAES system located 5 km off-shore with air stored at a depth of 100 m below water surface, an averaged, preferred optimal system design was determined to use a power input of 1967 kW, three air compression stages, a 340 mm header pipe, three expansion stages and a charge-discharge time ratio of 1.0.

## **2.0 RECOMMENDATIONS**

The findings of the studies performed mainly serve as recommendations to the development of future UWCAES systems. As UWCAES is currently under development, the information presented in this thesis provides valuable insights based on engineering fundamentals to the novel system concept. While the analyses performed captured the general operating characteristics and performance of UWCAES systems, a few recommendations can be made to further enhance the completed analyses.

In general, the systems modelled can be extended to include greater detail in components and subcomponents. Simplifications were made for a few elements as the analyses were conducted on a high-level. Integrating a lower-level examination of major components – such as the air compressor and turbo-expander – can increase the

accuracy of the results. However, it should be noted that certain components, like the ones aforementioned, might rely on proprietary and confidential information only available to component manufacturers.

The exergoeconomic analysis and optimization discussed in Chapter 4 can be further improved using higher quality equipment cost information. The cost functions applied in the study were sourced from past literature and updated with a limited manufacturer data. Instead, subsequent models could use cost information sourced from commercial cost estimating tools and software.

Sub-optimization routines can be used on UWCAES components to determine their optimum design/selection in the optimized system. The evaluation conducted in Chapter 4 focused on the top system-level, with components like the heat exchangers being designed based on constant properties. This can lead to improved optimization results, but may significantly increase computational expenses.

Lastly, optimization should continually be performed on evolving UWCAES designs that implement new or alternative details, methods, or processes as our industrial partner realizes them. Innovations in the system process or components typically lead to enhancing overall performance; optimization is a useful tool in studying the innovations to assess feasibility. Ongoing innovation is key to the long-term success and competitiveness of UWCAES in a growing energy storage market.



## APPENDIX A

### **PERMISSIONS FOR PREVIOUSLY PUBLISHED WORKS**

#### **CHAPTER II: DISTENSIBLE AIR ACCUMULATORS AS A MEANS OF ADIABATIC UNDERWATER COMPRESSED AIR ENERGY STORAGE**

As specified by the Taylor & Francis Group's Copyright and Authors Rights<sup>1</sup>, the publication's author retains the right to include an article in a thesis, provided that acknowledgement to journal publication is made explicit.

#### **CHAPTER III: PARAMETERS AFFECTING SCALABLE UNDERWATER COMPRESSED AIR ENERGY STORAGE**

As the article has yet to be accepted, no permissions are required. Upon acceptance of article, the author retains the right to include article in a thesis in accordance to Elsevier's Author Rights and Responsibilities<sup>2</sup>.

#### **CHAPTER IV: MULTI-OBJECTIVE OPTIMIZATION OF AN UNDERWATER COMPRESSED AIR ENERGY STORAGE SYSTEM USING A GENETIC ALGORITHM**

As the article has yet to be accepted, no permissions are required. Upon acceptance of article, the author retains the right to include article in a thesis in accordance to Elsevier's Author Rights and Responsibilities.

---

<sup>1</sup> <http://journalauthors.tandf.co.uk/permissions/reusingOwnWork.asp> (Accessed Nov. 22, 13)

<sup>2</sup> <http://www.elsevier.com/journal-authors/author-rights-and-responsibilities> (Accessed Nov. 22, 13)

## APPENDIX B

### **PERFORMANCE EVALUATION OF PREFERRED SYSTEM CONFIGURATION**

The following tables present the energy, exergy, and exergoeconomic evaluations of the modelled UWCAES system (described in Chapter 4, Section 4.0) with the following preferred system configuration (interest rate of 10%):

- A power input of 1967 kW,
- Three air compression stages,
- A 320 mm header pipe,
- Three expansion stages, and a
- Charge-discharge time ratio of 1.0.

Please note that for Tables B-1 and B2 that a negative value for energy and exergy associated with work indicates its production/output from the system.

Table B-1 - Energy Analysis of Modelled system

|                           | Air             |                  |                      |                       |                       |                            | Glycol          |                  |                       | Specific Work (kJ/kg) |
|---------------------------|-----------------|------------------|----------------------|-----------------------|-----------------------|----------------------------|-----------------|------------------|-----------------------|-----------------------|
|                           | Inlet Temp. (K) | Outlet Temp. (K) | Inlet Pressure (kPa) | Outlet Pressure (kPa) | Mass Flow Rate (kg/s) | Pressure Loss in HEX (kPa) | Inlet Temp. (K) | Outlet Temp. (K) | Mass Flow Rate (kg/s) |                       |
| <b>Compressor 1</b>       | 281.15          | 364.26           | 101.33               | 226.67                | 7.39                  | --                         | --              | --               | --                    | 83.48                 |
| <b>Heat Exchanger 1</b>   | 364.26          | 285.15           | 226.67               | 226.66                | 7.39                  | 0.00                       | 281.15          | 360.10           | 2.38                  | --                    |
| <b>Compressor 2</b>       | 285.15          | 369.44           | 226.66               | 507.04                | 7.39                  | --                         | --              | --               | --                    | 84.67                 |
| <b>Heat Exchanger 2</b>   | 369.44          | 285.15           | 507.04               | 507.04                | 7.39                  | 0.00                       | 281.15          | 365.03           | 2.38                  | --                    |
| <b>Compressor 3</b>       | 285.15          | 369.44           | 507.04               | 1134.26               | 7.39                  | --                         | --              | --               | --                    | 84.67                 |
| <b>Heat Exchanger 3</b>   | 369.44          | 285.15           | 1134.26              | 1134.26               | 7.39                  | 0.00                       | 281.15          | 365.03           | 2.38                  | --                    |
| <b>Pipe (Charging)</b>    | 285.15          | 281.15           | 1134.26              | 1082.33               | 7.39                  | --                         | --              | --               | --                    | --                    |
| <b>Air Storage</b>        | 281.15          | 281.15           | 1082.33              | 1082.33               | --                    | --                         | --              | --               | --                    | --                    |
| <b>Thermal Storage</b>    | --              | --               | --                   | --                    | --                    | --                         | 363.39          | 361.31           | --                    | --                    |
| <b>Pipe (Discharging)</b> | 281.15          | 281.15           | 1082.33              | 1028.73               | 7.39                  | --                         | --              | --               | --                    | --                    |
| <b>Heat Exchanger 3</b>   | 281.15          | 357.69           | 1028.73              | 1028.73               | 7.39                  | 0.00                       | 361.31          | 285.29           | 2.38                  | --                    |
| <b>Expander 1</b>         | 357.69          | 295.70           | 1028.73              | 475.09                | 7.39                  | --                         | --              | --               | --                    | -62.27                |
| <b>Heat Exchanger 2</b>   | 295.70          | 358.59           | 475.09               | 475.08                | 7.39                  | 0.00                       | 361.31          | 299.26           | 2.38                  | --                    |
| <b>Expander 2</b>         | 358.59          | 296.44           | 475.08               | 219.40                | 7.39                  | --                         | --              | --               | --                    | -62.43                |
| <b>Heat Exchanger 1</b>   | 296.44          | 358.55           | 219.40               | 219.39                | 7.39                  | 0.00                       | 361.31          | 300.05           | 2.38                  | --                    |
| <b>Expander 3</b>         | 358.55          | 296.41           | 219.39               | 101.32                | 7.39                  | --                         | --              | --               | --                    | -62.42                |

Table B-2 – Exergy Analysis of Modelled System

|                           | Air           |                | Glycol        |                | Work<br>(Electricity)<br>(kW) | Exergy<br>Destruction<br>(kW) |
|---------------------------|---------------|----------------|---------------|----------------|-------------------------------|-------------------------------|
|                           | Inlet<br>(kW) | Outlet<br>(kW) | Inlet<br>(kW) | Outlet<br>(kW) |                               |                               |
| <b>Compressor 1</b>       | 0.00          | 556.93         | --            | --             | 617.34                        | 60.41                         |
| <b>Heat Exchanger 1</b>   | 556.93        | 480.59         | 0.00          | 69.93          | --                            | 6.41                          |
| <b>Compressor 2</b>       | 480.59        | 1046.38        | --            | --             | 626.13                        | 60.34                         |
| <b>Heat Exchanger 2</b>   | 1046.38       | 961.01         | 0.00          | 78.45          | --                            | 6.92                          |
| <b>Compressor 3</b>       | 961.01        | 1526.80        | --            | --             | 626.13                        | 60.34                         |
| <b>Heat Exchanger 3</b>   | 1526.80       | 1441.43        | 0.00          | 78.45          | --                            | 6.92                          |
| <b>Pipe (Charging)</b>    | 1441.43       | 1413.28        | --            | --             | --                            | 28.16                         |
| <b>Air Storage</b>        | 1413.28       | 1413.28        | --            | --             | --                            | --                            |
| <b>Thermal Storage</b>    | --            | --             | 75.61         | 71.99          | --                            | 4.05                          |
| <b>Pipe (Discharging)</b> | 1413.28       | 1382.98        | --            | --             | --                            | 30.30                         |
| <b>Heat Exchanger 3</b>   | 1382.98       | 1448.63        | 71.99         | 0.22           | --                            | 6.12                          |
| <b>Expander 1</b>         | 1448.63       | 924.61         | --            | --             | -460.49                       | 63.53                         |
| <b>Heat Exchanger 2</b>   | 924.61        | 989.07         | 71.99         | 4.03           | --                            | 3.50                          |
| <b>Expander 2</b>         | 989.07        | 463.89         | --            | --             | -461.64                       | 63.54                         |
| <b>Heat Exchanger 1</b>   | 463.89        | 528.00         | 71.99         | 4.38           | --                            | 3.50                          |
| <b>Expander 3</b>         | 528.00        | 2.86           | --            | --             | -461.60                       | 63.54                         |

Table B-3 – Exergoeconomic Analysis of Modelled System (Cost Per Unit Exergy)

|                           | Air               |                    | Glycol            |                    | Work<br>(Electricity)<br>(\$/MWh) |
|---------------------------|-------------------|--------------------|-------------------|--------------------|-----------------------------------|
|                           | Inlet<br>(\$/MWh) | Outlet<br>(\$/MWh) | Inlet<br>(\$/MWh) | Outlet<br>(\$/MWh) |                                   |
| <b>Compressor 1</b>       | 0.00              | 39.07              | --                | --                 | 14.48                             |
| <b>Heat Exchanger 1</b>   | 39.07             | 39.07              | 0                 | 223.55             | --                                |
| <b>Compressor 2</b>       | 39.07             | 38.87              | --                | --                 | 14.48                             |
| <b>Heat Exchanger 2</b>   | 38.87             | 38.87              | 0                 | 206.49             | --                                |
| <b>Compressor 3</b>       | 38.87             | 38.81              | --                | --                 | 14.48                             |
| <b>Heat Exchanger 3</b>   | 38.81             | 38.81              | 0                 | 206.44             | --                                |
| <b>Pipe (Charging)</b>    | 38.81             | 51.44              | --                | --                 | --                                |
| <b>Air Storage</b>        | 51.44             | 121.14             | --                | --                 | --                                |
| <b>Thermal Storage</b>    | --                | --                 | 212.16            | 327.45             | --                                |
| <b>Pipe (Discharging)</b> | 121.14            | 121.14             | --                | --                 | --                                |
| <b>Heat Exchanger 3</b>   | 121.14            | 131.32             | 327.45            | 327.45             | --                                |
| <b>Expander 1</b>         | 131.32            | 131.32             | --                | --                 | 163.15                            |
| <b>Heat Exchanger 2</b>   | 131.32            | 144.75             | 327.45            | 327.45             | --                                |
| <b>Expander 2</b>         | 144.75            | 144.75             | --                | --                 | 176.51                            |
| <b>Heat Exchanger 1</b>   | 144.75            | 167.99             | 327.45            | 327.45             | --                                |
| <b>Expander 3</b>         | 167.99            | 167.99             | --                | --                 | 199.75                            |

Table B-4 – Exergoeconomic Evaluation of Modelled System (Cost Rate)

|                           | Air             |                  | Glycol          |                  | Work<br>(Electricity)<br>(\$/h) | Exergy<br>Destruction<br>(\$/h) | Capital<br>Cost<br>(\$/h) |
|---------------------------|-----------------|------------------|-----------------|------------------|---------------------------------|---------------------------------|---------------------------|
|                           | Inlet<br>(\$/h) | Outlet<br>(\$/h) | Inlet<br>(\$/h) | Outlet<br>(\$/h) |                                 |                                 |                           |
| <b>Compressor 1</b>       | 0               | 21.76            | --              | --               | 8.94                            | 2.36                            | 15.18                     |
| <b>Heat Exchanger 1</b>   | 21.76           | 18.78            | 0               | 15.63            | --                              | 1.43                            | 14.08                     |
| <b>Compressor 2</b>       | 18.78           | 40.68            | --              | --               | 9.07                            | 2.35                            | 15.18                     |
| <b>Heat Exchanger 2</b>   | 40.68           | 37.36            | 0               | 16.20            | --                              | 1.43                            | 14.31                     |
| <b>Compressor 3</b>       | 37.36           | 59.26            | --              | --               | 9.07                            | 2.34                            | 15.18                     |
| <b>Heat Exchanger 3</b>   | 59.26           | 55.95            | 0               | 16.19            | --                              | 1.43                            | 14.31                     |
| <b>Pipe (Charging)</b>    | 55.95           | 72.70            | --              | --               | --                              | 1.45                            | 18.20                     |
| <b>Air Storage</b>        | --              | --               | --              | --               | --                              | --                              | --                        |
| <b>Thermal Storage</b>    | --              | --               | --              | --               | --                              | --                              | --                        |
| <b>Pipe (Discharging)</b> | 171.21          | 167.54           | --              | --               | --                              | 3.67                            | --                        |
| <b>Heat Exchanger 3</b>   | 167.54          | 190.24           | 23.57           | 0.07             | --                              | 0.80                            | --                        |
| <b>Expander 1</b>         | 190.24          | 121.42           | --              | --               | -75.13                          | 10.37                           | 16.68                     |
| <b>Heat Exchanger 2</b>   | 121.42          | 143.17           | 23.57           | 1.32             | --                              | 0.51                            | --                        |
| <b>Expander 2</b>         | 143.17          | 67.15            | --              | --               | -81.48                          | 11.22                           | 16.68                     |
| <b>Heat Exchanger 1</b>   | 67.15           | 88.70            | 23.57           | 1.43             | --                              | 0.59                            | --                        |
| <b>Expander 3</b>         | 88.70           | 0.48             | --              | --               | -92.20                          | 12.69                           | 16.68                     |

## VITA AUCTORIS

NAME: Brian C. Cheung

PLACE OF BIRTH: Windsor, Ontario, Canada

YEAR OF BIRTH: 1989

EDUCATION: Vincent Massey Secondary School, Windsor, ON  
2003 – 2007  
University of Windsor, Windsor, ON  
2007 – 2011, B.A.Sc. Civil Engineering Co-op